A STUDY OF SOME EARLY-TYPE CLOSE BINARY STARS*

K. D. ABHYANKAR
Berkeley Astronomical Department, University of California
Received December 1, 1958

ABSTRACT

A study of spectroscopic and photometric material for three binaries has supplied additional evidence regarding dynamical interaction between their components.

1. *Beta Scorpii.*—A new orbit of the primary confirms the apsidal motion found by earlier workers. The γ velocity for the secondary is 40 km/sec positive with respect to that of the primary; at least part of the difference is real. λ 4471 of He I and λ 4553 of Si III are about twice as strong when the secondary is approaching as when the secondary is receding. Hγ shows smaller changes in the opposite direction. Changes in line intensities and the difference between γ_1 and γ_2 are attributed to gaseous matter projected against the approaching side of the secondary. Measured difference in the magnitudes of the two components indicates that the secondary is overluminous.

2. *HD 47129.*—Combining new observations with the old, a correct period of 14.3961 days is established, and a new orbit of the primary is obtained. The measures of secondary lines show large scatter, difference in γ_1 and γ_2, and a velocity amplitude smaller than the primary. Systematic changes in velocity-curves and line intensities from one epoch to the next are also noted. At phases around 7.2 days, the secondary lines are stronger by 30–40 per cent; hydrogen lines in the primary spectrum are fuzzy and have negative velocities with respect to the mean for all lines. The spectral types of the two components are alike, but the strength of the red He I lines indicates a strong red continuum for the secondary. Analysis of the shell lines gives a mean distance of the circumstellar envelope from the center of the primary equal to six times the radius of the star. Variations in the number of absorbing atoms in the envelope in different directions and from cycle to cycle are indicated. The electron temperature of the shell is 24000°, the electron density is 1.7×10^{11}/cc, and the mass density is about 3.3×10^{-13} gm/cc. The He/H abundance ratio in the primary is normal. The distance of the star is about 1140 parsecs.

3. *AO Cassiopeiae.*—Comparison of a new spectroscopic orbit with earlier orbits gives definitive values of $\gamma_1 = -31.1 \pm 0.07$ km/sec and $e = 0.035 \pm 0.004$. K_1 and K_2 seem to vary from epoch to epoch. Apsidal motion with a period of 70 years is found. Observations of the secondary are widely scattered, but they do not indicate any real difference between the γ velocities of the two components. The velocity amplitude of the secondary is smaller than that of the primary. Photometric light-curves in yellow, blue, and ultraviolet colors show asymmetries and negative reflection effects. The observed primary minimum is shifted by -0.67 day with respect to the computed phases. Irregular fluctuations of light of the order of 0.03 mag. are superposed on the smooth variation of the light of the primary.

I. INTRODUCTION

Close binaries of early spectral type, on account of their large masses and consequent rapid time scale of evolution, supply useful information regarding the dynamical interaction between the two components, as manifested by the presence of emission lines and peculiarities in the absorption lines in the spectra of these stars. Starting from β Lyr (Kuiper 1941; Struve 1941), the hypothesis of gaseous streams has provided a successful explanation of the observed phenomena in many binaries, such as U Cep, SX Cas, UX Mon, and others. But thus far a generalization of working models has not been possible. The principal aim of this investigation was to obtain additional evidence of interaction between the components of close binary stars from the study of several close binary systems of early spectral type. A routine check of the orbits was another purpose of the present study. Finally, an attempt was made to determine the H/He abundance ratio in a star of very early type, which is a member of a binary system.

* Thesis submitted in partial fulfilment of the requirements for the degree of Ph.D. in astronomy at the University of California.

II. OBSERVATIONAL MATERIAL

Selection of Binaries

Table 1 lists the ten binaries from the fifth catalogue of Moore and Neubauer (1948), north of $-25°$ and brighter than 6.5 mag., which have the largest orbital angular momenta and the largest kinetic energy. All the better-observed binaries in this list are known to be peculiar in one way or another. We should expect that the less observed stars, such as Boss 5629, ζ CrB A, and Boss 6142, may also be found to be peculiar from further observations. Of the remaining seven stars, α Vir and β Lyr have been observed quite extensively, while δ Ori and 29 CMa were observed recently by Stone (1956) and by Struve *et al.* (1958), respectively. The present observing program was limited to the

TABLE 1

O AND B-TYPE SPECTROSCOPIC BINARIES WITH LARGEST TOTAL ORBITAL ANGULAR MOMENTA AND LARGEST KINETIC ENERGIES

Star	Fifth Catalogue No.	Total Orbital Angular Momentum* (C.G.S. Units)	Total Kinetic Energy* (C.G.S. Units)	Group
HD 47129...	136	240×10^{53}	600×10^{47}	a
α Vir.....	207	56	525	a
β Lyr.....	356	72	225	a
29 CMa.....	146	20	172	b
AO Cas.....	6	15	158	b
Boss 5629....	440	27	60	b
δ Ori.....	106	11	75	c
ζ CrB A.....	284	16	45	c
β Sco.....	290	11	60	c
Boss 6142....	479	14	41	c

* These are lower limits obtained by putting $\sin i = 1$ and $\mathfrak{M}_1 = \mathfrak{M}_2$.

following three binaries: Plaskett's star HD 47129, AO Cas, and β Sco. It might be noted that they belong to groups a, b, and c of Table 1. In the order quoted, these groups represent decreasing amounts of kinetic energy and angular momentum of the system.

Observations

The three selected binaries were observed from June, 1956, to February, 1958. About 170 plates were obtained on 79 nights with the Mills spectrograph of the Lick Observatory. They were supplemented by about 50 plates obtained by Dr. Struve and Dr. Sahade at Mount Wilson. The Lick plates (LS) covered the spectral region from Hγ to λ 4713 of He I with a dispersion of 10 A/mm. The Mount Wilson coudé (Cd) plates had also a dispersion of 10 A/mm, but they covered a larger spectral region, from λ 3700 to Hβ. The Mount Wilson Cassegrain (Xd) plates had a dispersion of 20 A/mm and covered the region from λ 3700 to λ 4500. All plates were measured on a conventional measuring engine, and some were microphotometered with the simultaneous density-intensity recorder of the Leuschner Observatory.

Plaskett's star and AO Cas were also observed photoelectrically with the Tauchmann telescope of the Lick Observatory. Observations were made in three colors, using *Vl*, *Bl*, and *Ul* filters of the Lick system (Hogg and Kron 1955). AO Cas was observed on 27 nights, with BD+47°50 as the principal comparison star, while BD+51°62 was used

as a check star. Plaskett's star was observed on 14 nights; HD 47240 and HD 48099 were used as the primary and the secondary comparison stars. The extinction was determined for each night separately. The results for Plaskett's star were reported in an earlier paper (Abhankar and Spinrad 1958).

III. BETA SCORPII

β Sco is a visual triple star with a close companion about 1″ away and a distant one about 14″ away. According to measurements by Kuiper (1935), the apparent magnitudes of the close pair are 2.9 and 5.3; from the membership in the Scorpio-Centaurus cluster of B stars, Blaauw (1946) found absolute magnitudes of −3.79 and −1.28 for them. The binary character of the brighter star (MK type B0.5 V) was discovered by Slipher (1903). Orbits were computed by Duncan (1912) and by Daniel and Schlesinger

TABLE 2

LIST OF LINES MEASURED IN THE SPECTRUM OF β SCO

Wave Length (A)	Identification	Weight	
		Primary	Secondary
4340.468	H	1	2
4387.928	He I	1	2
4471.477	He I	1	2
4552.622	Si III	1	2
4567.841	Si III	1	1
4574.777	Si III	1	1
4590.98	O II	1	.....
4596.19	O II	1	.....
4641.811	O II	1	.....
4661.635	O II	1	.....
4685.682	He II	1	1
4713.20	He I	1	1
Mean weight for one plate		12	10
Internal p.e. for average plate		3.6 km/sec	10.2 km/sec
P.e. of an average line	Weight 1	12.5 km/sec	32.2 km/sec
	Weight 2	.....	22.8 km/sec

(1912). Luyten, Struve, and Morgan (1940) found a forward rotation of the line of apsides. The ratio U/P (the period of rotation of the apsidal line to the period of revolution of the binary) derived by them should be corrected to 32000 ± 4600. Photometric observations by Stebbins (1914) were not conclusive, but a slight eclipse was suspected. Petrie (1950) obtained spectrophotometrically $\Delta m = 1.25 \pm 0.10$ for the difference in the magnitudes of the components of the binary. Furthermore, Struve (1937) observed variations in the intensities of secondary lines which were strongest when the velocity of the secondary was negative.

The New Spectroscopic Orbit

The new orbit is based on 98 Mills plates; the lines of the secondary were measured on 71 plates. Table 2 gives the list of lines measured and weights attached to each of them. Table 3 contains the measured radial velocities of the two components. The orbits of both components were computed on the IBM 701 digital computer of the University of California's computer center, using the program written by Su-Shu Huang [Sahade *et al.* (1959)], which is based on Sterne's (1941) method for improving the elements of an

1959ApJS....4..157A

Table 3

Measured velocities of Beta Scorpii.

Date	Old phase	New phase	v_1 km/sec.	v_2 km/sec.
1956	Days	Days		
June 12, 7:30 UT	3.630	3.653	- 076.4	+ 218.1
June 13, 6:30	4.590	4.613	- 019.0	-----
7:12	4.618	4.641	- 028.5	-----
8:20	4.665	4.688	- 025.6	-----
June 17, 6:56	1.779	1.802	- 080.9	+ 171.2
7:52	1.818	1.841	- 088.7	+ 189.9
8:15	1.834	1.857	- 065.4	+ 189.1
June 21, 6:39	5.767	5.790	+ 082.4	- 184.9
7:10	5.789	5.812	+ 072.9	- 206.5
7:39	5.809	5.832	+ 086.1	- 172.2
June 22, 6:57	6.780	6.803	+ 162.0	- 168.7
7:24	6.799	6.822	+ 160.9	- 204.7
7:54	6.819	0.014	+ 146.6	- 173.9
June 26, 7:02	3.955	3.978	- 081.9	+ 191.4
7:34	3.978	4.001	- 061.9	+ 149.4
June 28, 6:26	5.930	5.953	+ 087.4	- 189.6
6:47	5.945	5.968	+ 090.6	- 168.2
7:16	5.965	5.988	+ 096.6	- 166.1
July 8, 5:37	2.239	2.263	- 112.3	+ 167.7
5:58	2.254	2.278	- 106.8	+ 185.6
6:19	2.268	2.292	- 101.0	+ 191.5
6:40	2.283	2.307	- 099.0	+ 177.0
July 9, 4:30	3.193	3.217	- 093.5	+ 186.4
4:53	3.208	3.232	- 105.5	+ 181.2
5:16	3.224	3.248	- 090.0	+ 192.6
5:40	3.241	3.265	- 091.3	+ 193.8
July 15, 4:28 UT	2.363	2.387	- 109.8	+ 180.6
4:57	2.383	2.407	- 105.4	+ 192.8
5:24	2.402	2.426	- 096.3	+ 210.4
5:51	2.421	2.445	- 091.4	+ 213.2
July 16, 4:28	3.363	3.387	- 079.1	+ 170.3
4:50	3.378	3.402	- 092.8	+ 208.5
5:16	3.396	3.420	- 086.8	+ 222.1
5:42	3.415	3.439	- 083.4	+ 227.6
Aug. 3, 4:11	0.867	0.890	+ 020.6	-----
4:38	0.886	0.909	+ 023.4	-----
5:11	0.909	0.932	+ 029.7	-----
Aug. 24, 3:46	1.365	1.389	- 022.7	-----
1957				
April 7, 9:35	2.279	2.302	- 090.9	+ 217.0
10:28	2.316	2.339	- 092.6	+ 217.8
11:15	2.349	2.372	- 099.2	+ 229.2
12:02	2.381	2.404	- 099.4	+ 222.3
May 29, 9:20	6.472	6.495	+ 153.9	- 166.3
May 30, 5:50	0.497	0.521	+ 111.3	- 135.4
7:15	0.556	0.580	+ 103.9	- 161.9
8:09	0.594	0.618	+ 088.1	- 172.8
June 6, 5:05	0.638	0.662	+ 083.2	-----
6:04	0.679	0.703	+ 077.8	-----
6:51	0.711	0.735	+ 065.5	-----
7:30	0.738	0.762	+ 069.2	-----
8:12	0.768	0.792	+ 062.9	-----

1959ApJS....4..157A

Table 3 (continued)

Date	Old phase	New phase	v_1 km/sec.	v_2 km/sec.
1957	Days	Days		
June 7, 5:05 UT	1.638	1.662	- 065.2	-----
5:51	1.670	1.694	- 069.0	-----
6:27	1.695	1.719	- 062.5	-----
7:03	1.720	1.744	- 073.0	-----
7:43	1.748	1.772	- 070.2	-----
June 8, 6:46	2.708	2.732	- 109.8	+ 201.2
7:28	2.737	2.761	- 105.0	+ 222.8
June 26, 4:48	0.142	0.166	+ 149.0	- 180.3
5:19	0.164	0.188	+ 148.6	- 195.0
5:56	0.189	0.213	+ 141.4	- 189.2
6:33	0.215	0.239	+ 146.9	- 183.3
7:17	0.245	0.269	+ 144.6	- 172.6
June 27, 4:39	1.136	1.160	+ 002.1	-----
5:13	1.159	1.183	- 008.9	-----
5:55	1.189	1.213	- 014.1	-----
6:28	1.211	1.235	- 015.2	-----
7:12	1.242	1.266	- 016.7	-----
July 2, 4:32	6.131	6.155	+ 109.2	- 168.4
5:03	6.152	6.176	+ 115.7	- 160.5
5:38	6.177	6.201	+ 113.7	- 163.7
6:18	6.204	6.228	+ 115.5	- 173.3
6:58	6.232	6.256	+ 118.3	- 188.6
July 3, 4:35	0.305	0.329	+ 141.5	- 142.0
5:15	0.333	0.357	+ 138.4	- 147.1
5:49	0.356	0.380	+ 141.8	- 147.4
6:21	0.379	0.403	+ 135.3	- 171.1
7:01	0.406	0.430	+ 127.3	- 164.8
July 15, 4:25	5.470	5.493	+ 033.1	-----
4:53	5.489	5.512	+ 038.6	- 157.9
5:28	5.514	5.537	+ 047.0	-----
6:10	5.543	5.566	+ 039.6	-----
July 16, 4:20	6.467	6.490	+ 138.4	- 186.4
4:49	6.487	6.510	+ 143.3	- 214.9
5:25	6.512	6.535	+ 137.0	- 188.9
6:07	6.541	6.564	+ 143.4	- 191.5
July 19, 4:21	2.638	2.662	- 102.4	+ 211.7
4:54	2.661	2.685	- 105.8	+ 216.0
5:28	2.685	2.709	- 105.1	+ 187.9
6:03	2.709	2.733	- 104.0	+ 177.0
July 30, 4:05	6.799	6.823	+ 159.8	- 209.5
4:33	6.819	0.015	+ 153.3	- 180.5
5:10	0.016	0.040	+ 154.6	- 193.3
Aug. 2, 4:03	2.970	2.994	- 101.8	+ 226.0
4:32	2.990	3.014	- 096.1	+ 239.7
5:09	3.016	3.040	- 097.9	+ 233.1
Aug. 4, 4:12	4.976	5.000	+ 009.7	-----
4:56	5.007	5.031	- 001.9	-----

Table 4

Orbits of Beta Scorpii.

Element etc.	Units	Lowell Duncan 1908-12	Allegheny Daniel and Schlessinger 1911	Yerkes Luyten, Struve & Morgan 1934-36	Lick Abhyankar 1956-57		
Mean epoch	Periods	0	106	1433	2450		
n_1	No. of plates	90	73	94	98		
n_2	No. of plates	--	30	26	71		
					701 soln. for secondary	soln. for γ_2 & K_2	soln. for K_2 only
e_1		0.27	0.270±.0085	0.262±.008	----------	0.276±.005	---------
e_2		0.27	0.270	0.262	0.080±.017	0.276	0.276
K_1	km/sec.	126	125.7±1.2	126.0±0.8	----------	129.0±0.6	---------
K_2	km/sec.	166	197±10.5	212± 7	212.7±2.3	215.2±3.6	208.0±8.9
γ_1	km/sec.	- 8.0	- 11.0	- 3.8±0.7	----------	- 1.0±0.5	---------
γ_2	km/sec.	- 8.0	- 11.0	- 3.8±0.7	+ 19.3±3.5	+39.2±4.7	- 1.0
ω_1	degrees	20.0±1.7	20.1±2.2	35.0±1.6	----------	37.9±1.1	---------
ω_2	degrees	200	200.1	215	235±22	217.9	217.9
T_p 1	JD 2400000 +	18501.562	19225.378	28286.484	---------	35845.228±.022	-------
2	JD 2400000 +	18501.562	19225.378	28286.484	35845.444±.282	--- 35845.228	-----
T_Ω 1	JD 2400000 +	18501.349 ±.008	19225.165 ±.010	28286.098 ±.008	---------	35844.823±.007	-------
T_Ω $(O-C)_{old}$	days	- 0.017	+ 0.015	0.000		- 0.032	
T_Ω $(O-C)_{new}$	days	- 0.019	+ 0.015	+ 0.013		- 0.008	
$a_1 \sin i$	10^6 km.	10.99	11.36	11.4	----------	11.64	---------
$a_2 \sin i$	10^6 km.	14.45	17.80	19.2	19.91	19.42	18.77
$m_1 \sin^3 i$	solar masses	9.0	13.0	15.4	16.5	16.0	
$m_2 \sin^3 i$	solar masses	6.8	8.3	9.2	10.0	9.6	9.9
m_1 / m_2		1.32	1.57	1.67	1.65	1.67	1.61
p.e. of one plate....	km/sec.	5.7	8.0	5.8	----------	4.5	---------
	km/sec.	---	---	---	17.0	26.2	65.5

approximate orbit. The machine carries out successive least-squares solutions until the corrections become smaller than the mean errors of the various unknowns. The final elements and their probable errors are given in Table 4, which also includes the elements obtained by earlier workers. The three entries for the secondary in the Lick column correspond to the following three solutions: (1) 701 free solution, all five elements were computed without regard to the solution for the primary; (2) e, ω, and T_0 were taken over from the primary solution and only γ and K computed for the secondary; and (3) even γ_2 is put equal to γ_1 and only K_2 computed. Figure 1 shows the observed points and computed curves for the radial velocities of the two components; solution 2 for the secondary is represented.

a) Discussion of results for the primary.—1. Velocity of the system: There is a systematic change in the value of γ_1 from 1910 through 1935 to 1956–1957. The difference is

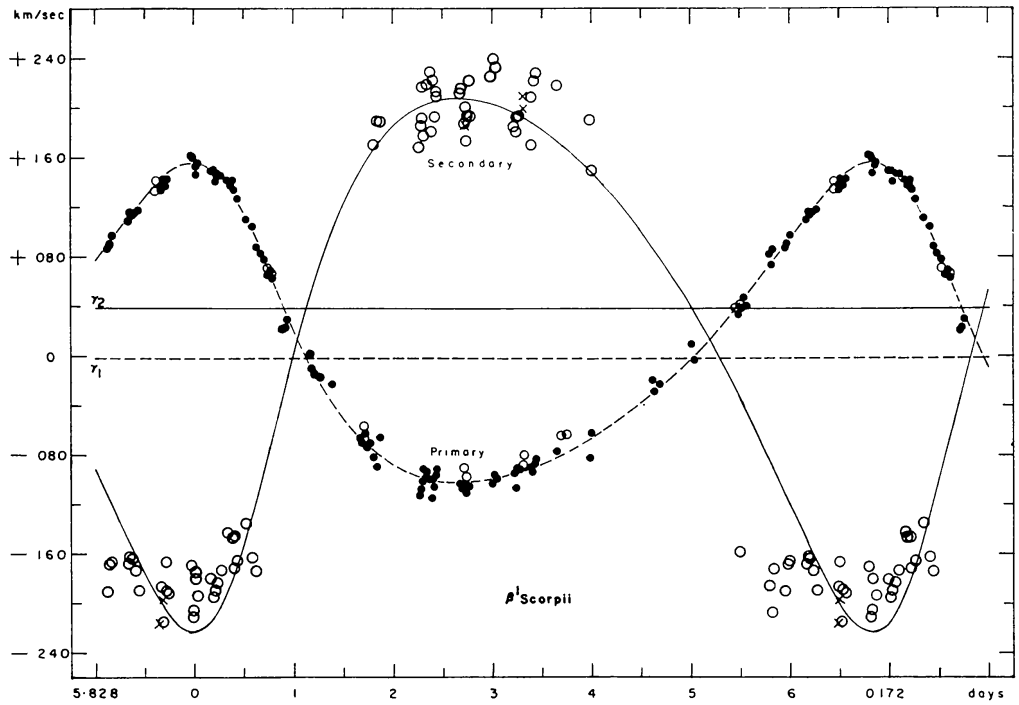

FIG. 1.—The radial velocity-curves for β Sco. Open circles (primary) and crosses (secondary) represent measures on more recent Mount Wilson plates.

small and may be due mainly to the differences in the velocity systems. But if the systematic nature of the change is the effect of the close visual companion, it is not possible at present to derive the visual orbit or to predict the expected change in radial velocity, because the visual observations from 1890 to 1950 cover only a small arc of about 30°.

2. The period: From the expression for the times of nodal passage derived by Luyten, Struve, and Morgan (1940) a residual (O−C) = −0.032 day is obtained for the present series of observations, which is rather large compared to the probable error of 0.007 day. Therefore, a least-squares solution was made to improve the epoch and period:

$$T_\Omega = \text{JD}2418501.368 \pm 0.008 + (6.828135 \pm 0.000002)E\,.$$

The new residuals T_Ω(O−C) given in Table 4 are reasonable for all four series of observations. The upper part of Figure 2 shows the fit of the observed T_Ω with the new period (*solid line*).

3. Apsidal motion: A least-squares solution which takes into account the probable errors of ω in the four available solutions of the orbit, gives the following ephemeris for ω:

$$\omega = 21^{\circ}.0 \pm 1^{\circ}.7 + (0^{\circ}.00706 \pm 0^{\circ}.00090)E .$$

It corresponds to $U/P = 51000 \pm 6500$, which means that the rotation of the line of apsides is somewhat slower than what was found by earlier workers. The lower part of Figure 2 represents the observations. Finally, putting $\mathfrak{M}_1/\mathfrak{M}_2 = 1.67$, $R_1/r = \frac{1}{5}$, and $R_2/r = \frac{1}{6}$ in the equation

$$\frac{P}{U} = k_1\left(\frac{R_1}{r}\right)^5\left(1+16\,\frac{\mathfrak{M}_2}{\mathfrak{M}_1}\right)+k_2\left(\frac{R_2}{r}\right)^5\left(1+16\,\frac{\mathfrak{M}_1}{\mathfrak{M}_2}\right), \qquad (1)$$

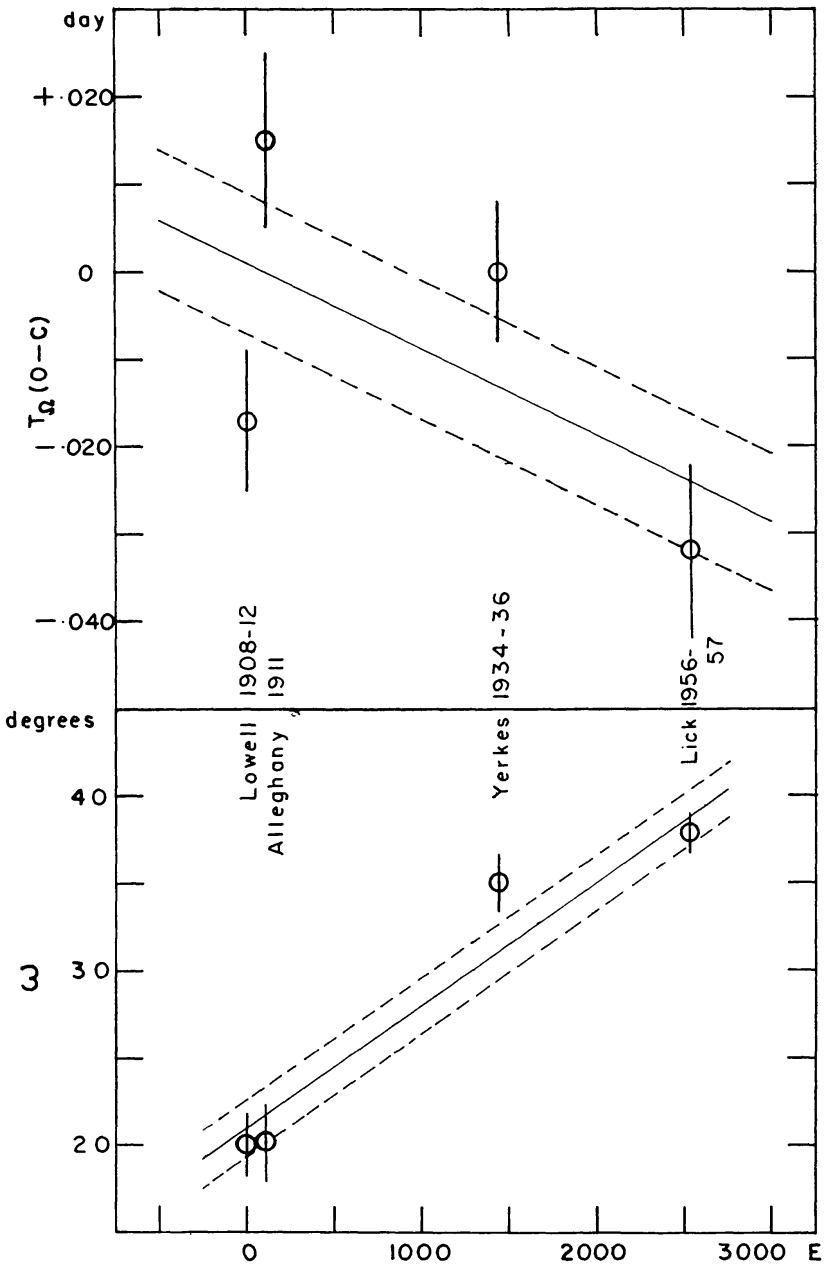

FIG. 2.—*Top:* correction to the period of β Sco; *bottom:* apsidal motion in β Sco

we derive $k_1 = k_2 = 0.00282$, which corresponds to a polytropic index between 3 and 4.

b) Discussion of results for the secondary.—In solution 1 the orbit of the secondary was computed independently; therefore, there is no guaranty that it would be consistent with the primary orbit. From entries in Table 4 we find that ω and T_p for the secondary are in fair agreement with the primary elements but that e and γ_2 are quite discordant. Since the points for the secondary are not sufficiently well distributed, the eccentricity derived from the free solution is not reliable. Hence, in solution 2, e, ω, and T_p are taken from the primary orbit, and γ_2 and K_2 only are computed. In this case the value of K_2 is not substantially different from solution 1; but γ_2 is now changed to $+39.2 \pm 4.7$ km/sec from its value of $+19.3 \pm 3.5$ km/sec in solution 1. Both values are more positive than the γ velocity for the primary. If we forcibly make γ_2 equal to γ_1, as is done in solution 3, K_2 is still not much different from the other solutions; but now the probable error of a single plate (65.5 km/sec) is too large compared to the internal probable error of an average plate (10.5 km/sec) or even the probable error of an average line (Wt. 2) on an average plate (22.8 km/sec). It appears that the measures do indicate a difference between γ_1 and γ_2, in the sense that γ_2 is larger than γ_1.

Systematic errors of measurement cannot be completely ruled out; this question will be discussed further in connection with the observations of AO Cas. Here it will be noted that the earlier workers did not find any difference between γ_2 and γ_1. But it is significant that Duncan obtained $K_2 = 166$ km/sec, while Daniel and Schlesinger, whose observations were not far removed in time from those of Duncan, found $K_2 = 197$ km/sec. We feel that the observed difference in γ_1 and γ_2 is at least partly real. If this is an effect of gaseous streams in the system, it is probably related to the phenomena of changes in the intensity of the secondary lines reported by Struve (1937).

In Figure 1, open circles (primary) and crosses (secondary) represent measures on Mount Wilson coudé plates recently obtained by Dr. Struve. They confirm the results from the Lick material.

IV. INTENSITIES OF SECONDARY LINES

Petrie's Method

Petrie's method for determining the difference in magnitude of the components of a spectroscopic binary was described in detail by Petrie (1939); here some of his formulae are put in a slightly different form to make them suitable for removing the effect of the secondary star from the observed equivalent widths and depths of the primary lines.

Let I_1 and I_2 be the contributions of the primary and secondary star, respectively, to the intensity at a particular point in the line at single-line phase. Let I_1^c and I_2^c be the corresponding intensities in the adjacent continuum. Then the observed depth $\mathfrak{R}'$ at the point under consideration is related to the true depths, $\mathfrak{R}_1$ and $\mathfrak{R}_2$, of the primary and secondary lines, respectively, by the relation

$$\mathfrak{R}' = \frac{\mathfrak{R}_1}{1 + I_2^c/I_1^c} + \frac{\mathfrak{R}_2 I_2^c/I_1^c}{1 + I_2^c/I_1^c}.$$

Suppose that $I_2^c = lI_1^c$, and $\mathfrak{R}_2 = k\mathfrak{R}_1$. Then

$$\mathfrak{R}' = \frac{1 + lk}{1 + l}\,\mathfrak{R}_1. \tag{2a}$$

On integrating over the wave length, we have

$$W' = \frac{1 + lk}{1 + l}\,W_1, \tag{2b}$$

where W' is the observed equivalent width of the combined line and W_1 is the true equivalent width of the primary line.

When the lines are separated, we have

$$\mathfrak{R}_1' = \frac{\mathfrak{R}_1}{1+l} \quad \text{and} \quad \mathfrak{R}_2' = \frac{\mathfrak{R}_1 lk}{1+l}, \tag{3a), (3b)}$$

$$W_1' = \frac{W_1}{1+l} \quad \text{and} \quad W_2' = \frac{W_1 lk}{1+l}, \tag{4a), (4b)}$$

where the primes represent the observed quantities and the true quantities are unprimed. Equations (3) and (4) further give

$$\frac{\mathfrak{R}_2'}{\mathfrak{R}_1'} = lk \quad \text{and} \quad \frac{W_2'}{W_1} = lk\,. \tag{5a), (5b)}$$

Formulae (5*a*) and (5*b*) are Petrie's (1939) formulae (7) and (11), respectively. He has also derived equations giving lk when the two lines overlap. His equations (6)—profile—and (12)—total absorption—apply to cases where the overlapping components are non-separable; and his equations (5)—profile—and (10)—absorption—apply when they overlap but are separable. It is usually difficult to decide whether a particular set of lines is separable or non-separable. Hence in the profile method the results from equations (5) and (6) were averaged; and, when considering total absorption, the results from equations (10) and (12) were averaged.

The factor k can be different from unity under three conditions: (i) When the spectral types of the two components are different. In this case the value of k will differ from line to line, and also the value of l will vary systematically with wave length. (ii) When rotation, macroturbulence, or pressure broadening affects the two stars differently. In this case, if the two stars have the same spectral type, the absorption formulae, viz., equation (5*b*) of this paper and Petrie's equations (10) and (12), will still be valid with $k = 1$. (iii) When different amounts of gaseous material are projected against the disks of the two stars. This will be observed as a change of lk with phase.

Application to β Sco

Microphotometer tracings were made for 14 plates of double-line phases taken on six nights and two plates of single-line phases taken on two nights. A mean profile was obtained for each night with double lines, and it was compared with the mean profile for the two nights with single lines. The results for Hγ and λ 4388 and λ 4471 of He I are assembled in Table 5. The following conclusions can be drawn:

a) The value of lk obtained from He I lines is, on an average, only slightly larger than that from Hγ. Therefore, there is little difference in the spectral types of the two components, a conclusion in agreement with Petrie's (1950) results.

b) λ 4471 of He I shows a marked change in lk with phase from about 0.2, when the primary is approaching, to about 0.4, when the primary is receding. Thus Struve's (1937) visual observations are confirmed. Hγ shows a smaller change in the opposite sense, i.e., the line is somewhat weaker when the primary is receding, a result similar to that found by Inglis (1956) in the spectroscopic binary π Sco.

c) Since the spectral types of the two components are alike, we assume that $k = 1$ and thus obtain a mean $l = 0.37 \pm 0.01$, or $\Delta m = 1.09 \pm 0.03$. Comparing with Petrie's (1950) result, $\Delta m = 1.25 \pm 0.10$, we adopt a mean $\Delta m = 1.15 \pm 0.05$. This spectroscopic difference between the magnitudes of the two components is too small for the mass ratio of 1.67 indicated by the orbits of 1934–1936 and 1956–1957. The secondary is overluminous by about 1 mag.

Table 5

Values of ℓk for lines of Beta Scorpii

I	II		III	IV	V	VI	VII	VIII	IX	X	XI
Date	Mean phase in days	Line.... Method.. Formulae	He I 4388			He I 4471			Mean He I	H	Mean for all lines.
			Absorption 5b	Cent. dep. 5a	Mean	Absorption Petrie (5)+(6)/2	Profile (10)+(12)/2	Mean		Absorption Petrie (10)+(12)/2	
1956 July 8, 5:37 UT	2.285		.485	.495	.490	.188	.264	.226	.358	.332	.349
6:40											
July 9, 4:30	3.241		.538	.515	.526	.168	.276	.222	.374	.389	.379
5:40											
July 16, 4:28	3.403		.490	.452	.471	.141	.202	.172	.322	.496	.380
4:50											
5:16											
June 21, 6:39	5.811		.299	.385	.342	.419	.216	.318	.330	.274	.311
7:10											
7:39											
June 28, 6:26	5.961		.333	.418	.376	.582	.345	.464	.420	.266	.369
6:47											
June 22, 6:57	6.823		.532	.476	.504	.415	.431	.423	.464	.309	.412
7:54											
Mean					.452			.304	.378	.344	.367±.010
Δm					0.862			1.293	1.056	1.159	1.088±.030

Visual Estimates

The ratio of the intensities of the primary and secondary lines was estimated visually on all plates which showed two lines. Estimates for Hγ, λ 4388 and λ 4471 of He I, and λ 4553 of Si III are plotted as functions of phase in Figure 3. The results for Hγ are not reliable because of rapid fading of the Mills spectrum in its vicinity. The correlation between estimated and measured intensity ratios is fairly good and positive for the two helium lines. Figure 3 shows the marked strengthening not only of λ 4471 of He I but also of λ 4553 of Si III at phases when the secondary is approaching. It is significant that the lower levels of both lines are metastable with respect to the ground level. Increase in

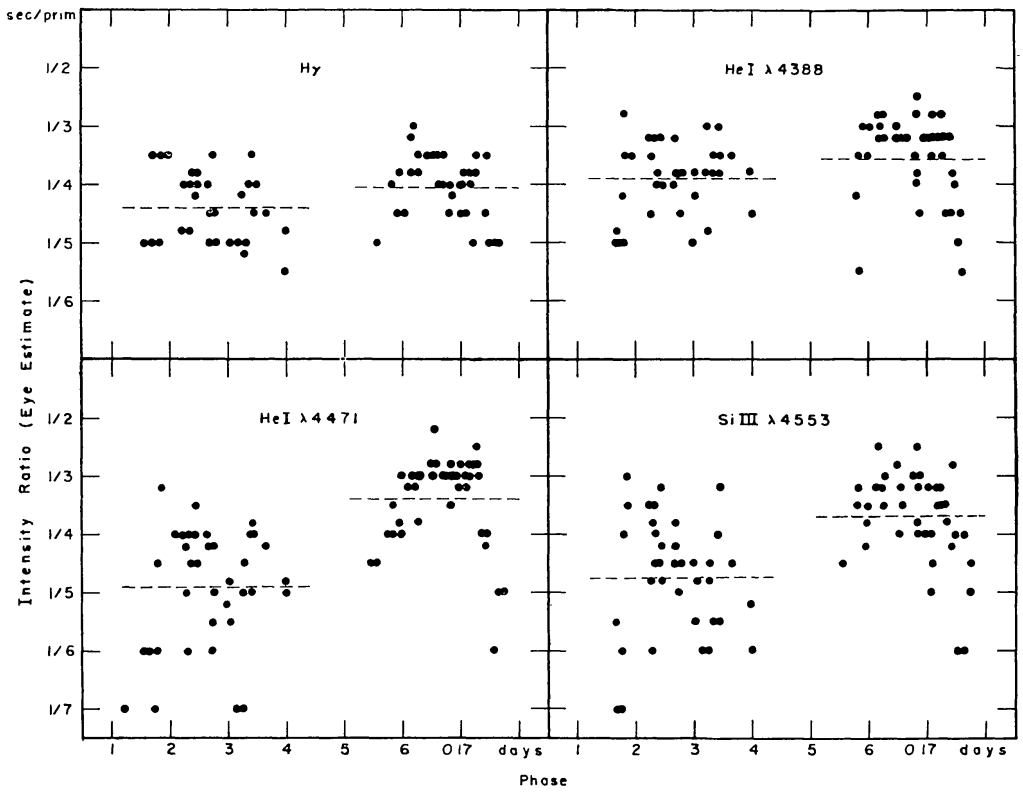

FIG. 3.—Visual estimates of intensity ratio for the lines of β Sco

their strength is very likely the effect of dilution, so that we might infer the presence of gaseous material projected in front of the approaching side of the secondary.

V. PLASKETT'S STAR

The binary nature of HD 47129 (MK type O8) was discovered by Plaskett (1922), who found the period to be 14.414 days. Struve (1948) reobserved the star in 1947 at the McDonald Observatory. He found that the velocity-curve was shifted by +2.6 days, γ_2 was smaller than γ_1 by about 100 km/sec, and the intensities of secondary lines changed with phase. Recently Struve, Sahade, and Huang (1958) found shell lines of He I and broad emission in Hα, both corresponding to a velocity of expansion of about 700 km/sec. Flow of material from the secondary toward the primary through the Lagrangian point, L_1, was indicated. They had also suggested that the secondary is perhaps a cool star of type A or F.

Photometric observations by Guthnick (1923*a*) and by Stebbins (1928) did not establish any variation in light; but Abhyankar and Spinrad (1958) find irregular fluctua-

Table 6

List of lines measured in the spectra of HD 47129 and A0 Cassiopeiae.

Wave length	Element	HD 47129 Plates	Weight for A0 Cas. LS	Cd	Xd	Wave length	Element	HD 47129 Plates	Weight for A0 Cas. LS	Cd	Xd
3587.252 A	He I	Cd	--	1	--	4097.31 A	N III	Cd	--	1	1
3613.641	He I	Cd	--	1	--	4101.737	H δ	Cd	--	1	1
3634.235	He I	Cd	--	1	--	4103.37	N III	Cd	--	--	--
3705.003	He I	Cd	--	1	1	4116.104	Si IV	Cd	--	1	1
3711.973	H 15	--	--	--	1	4120.812	He I	Cd	--	1	1
3721.940	H 14	--	--	--	1	4143.759	He I	Cd	--	1	1
3734.370	H 13	Cd	--	1	1	4199.83*	He II	Cd	--	1	1
3750.154	H 12	Cd	--	1	1	4200.02*	N III				
3754.62	N III	Cd	--	1	--	4340.468	H γ	Cd, LS	3	1	1
3759.87	O III	--	--	--	1	4379.09	N III	Cd, LS	2	1	1
3770.632*	H 11	Cd	--	1	1	4387.928	He I	Cd, LS	3	1	1
3771.08*	N III		--	--	--	4471.477	He I	Cd, LS	4	1	1
3791.26	O III	--	--	--	1	4510.92	N III	Cd, LS	2	1	--
3797.900	H 10	Cd	--	1	1	4514.89	N III	Cd, LS	2	1	--
3813.50	He II	Cd	--	--	--	4518.18	N III	Cd, LS	1	1	--
3819.606	He I	Cd	--	1	1	4523.60	N III	Cd, LS	1	1	--
3835.386	H 9	Cd	--	1	1	4534.57	N III	Cd, LS	1	--	--
3858.07	He II	Cd	--	--	--	4541.89	He II	Cd, LS	1	1	--
3867.477	He I	Cd	--	--	--	4546.36	N III	LS	--	--	--
3871.819	He I	Cd	--	--	--	4631.38	Si IV	LS	--	--	--
3888.646*	He I	Cd	--	1	1	4634.16	N III	------	2	1	--
3889.051*	H 8					4640.64	N III	LS	2	1	--
3923.48	He II	Cd	--	--	--	4654.14	Si IV	LS	--	--	--
3926.530	He I	Cd	--	--	--	4685.682	He II	Cd, LS	3	1	--
3964.727	He I	Cd	--	--	--	4713.143	He I	Cd, LS	3	1	--
3970.074	H ε	Cd	--	1	1	4861.332	H β	Cd	--	1	--
4009. 270	He I	Cd	--	--	--						
4026.189	He I	Cd	--	1	1	3933.664	Ca II K	Cd		1	1
4088.863	Si IV	Cd	--	1	1	3969.261	Ca II H	Cd		1	1

* The two lines on either side of the asterisks were measured as one.
LS--Lick plates; Cd--Mt. Wilson 100 inch coudé plates; Xd--Mt. Wilson 60 inch cassegrain plates.

Table 7a

Measured velocities of HD 47129.

Date	Phase in days.	v_1 km/sec.	v_2 km/sec.	Velocity of Ca II km/sec.
Lick plates:				
1956				
Oct. 20, 12:01 UT	08.979	+ 197.9	- 115.8	-----
Oct. 21, 11:54	09.974	+ 106.2	- 127.3	-----
Nov. 3, 11:51	08.576	+ 183.6	- 119.1	-----
Nov. 4, 11:31	09.562	+ 145.8	- 150.0	-----
Nov. 23, 9:37	14.086	- 161.2	+ 142.0	-----
12:31	14.207	- 156.2	+ 127.0	-----
Nov. 24, 10:38	00.732	- 147.5	+ 201.6	-----
Dec. 1, 11:17	07.759	+ 214.6	-----	-----
Dec. 20, 7:01	12.185	- 093.3	+ 174.0	-----
Dec. 21, 7:28	13.204	- 168.7	+ 139.8	-----
Dec. 23, 7:34	00.812	- 173.2	+ 115.3	-----
10:29	00.934	- 161.5	+ 122.4	-----
Dec. 24, 7:12	01.797	- 112.8	+ 228.8	-----
Dec. 25, 7:18	02.801	- 029.9	+ 317.2	-----
10:19	02.927	- 029.8	+ 226.8	-----
Dec. 26, 8:40	03.858	+ 046.8	- 197.3	-----
1957				
Jan. 27, 6:47	06.988	+ 241.4	- 147.4	-----
Feb. 9, 7:12	05.609	+ 180.2	- 088.3	-----
Mar. 17, 5:12	12.734	- 109.1	+ 141.3	-----
Oct. 31, 11:56	10.676	+ 030.5	-----	-----
Dec. 2, 10:11	13.811	- 183.6	+ 196.9	
Dec. 9, 10:02	06.409	+ 236.2	- 207.0	-----
1958				
Jan. 5, 8:31	04.553	+ 113.4	- 137.9	-----
Jan. 17, 5:43	02.040	- 088.5	+ 263.6	-----
Mar. 4, 5:13	04.831	+ 127.0	- 182.2	-----

Date	Phase in days.	v_1 km/sec.	v_2 km/sec.	Velocity of Ca II km/sec.
Mount Wilson 100 inch coudé plates:				
1956				
Nov. 21, 12:30 UT	12.206	- 099.0	+ 240.7	+ 18.81
Nov. 22, 12:24	13.202	- 155.9	+ 202.4	+ 17.65
1957				
Jan. 9, 10:57	03.557	+ 040.4	-----	+ 18.00
Jan. 17, 5:44	11.340	- 026.0	+ 234.2	+ 20.38
9:38	11.502	- 037.0	+ 290.2	+ 17.24
Jan. 18, 5:00	12.309	- 112.1	+ 155.4	+ 19.56
9:29	12.496	- 117.3	+ 236.8	+ 18.30
Mar. 21, 5:50	02.363	- 069.3	-----	+ 16.78
7:19	02.425	- 065.2	+ 269.9	+ 19.80
Apr. 9, 4:48	06.924	+ 230.2	- 165.9	+ 19.20
5:21	06.947	+ 228.1	- 173.2	+ 18.40
Apr. 10, 3:15	07.859	+ 216.3	- 133.0	+ 17.07
3:46	07.881	+ 225.2	- 182.6	+ 19.35
4:20	07.905	+ 224.9	- 198.1	+ 20.85
4:49	07.925	+ 217.7	- 149.0	+ 20.83
5:20	07.946	+ 222.1	- 202.3	+ 18.87
Apr. 11, 4:08	08.896	+ 181.9	- 196.5	+ 20.97
5:05	08.936	+ 180.5	- 176.5	+ 18.60
Apr. 12, 3:44	09.880	+ 112.8	- 186.7	+ 18.00
4:13	09.900	+ 112.3	- 226.4	+ 21.44

1959ApJS....4..157A

Corrected phases for Victoria and Mc Donald plates of HD 47129.

Victoria Plates		Mc Donald Plates					
Julian Date	Corrected phase	Date	Corrected phase	Date	Corrected phase	Date	Corrected phase
2423 040.949	09.079	1947					
053.838	07.572	Nov. 25, 6:50 UT	10.281	Dec. 5, 7:35 UT	05.916	Dec. 29, 8:35 UT	01.166
056.874	10.608	7:52	10.324	8:46	05.965	9:33	01.206
067.849	07.187	8:26	10.347	9:56	06.014	10:40	01.252
084.802	09.744	Nov. 26, 7:59	11.329	Dec. 6, 6:43	06.880	Dec. 30, 9:43	02.213
104.753	00.903	8:15	11.340	7:40	06.919	10:00	02.225
105.660	01.810			8:34	06.957		
106.802	02.952	Nov. 27 6:44	12.277			Dec. 31, 10:53	03.261
109.733	05.883	7:35	12.312	Dec. 7, 9:11	07.983	11:23	03.282
110.632	06.782	11:09	12.461	10:10	08.024		
				11:09	08.065	1948	
110.736	06.886	Nov. 28 6:14	13.256			Jan. 1, 7:11	04.107
111.675	07.825	6:34	13.270	Dec. 8, 9:56	09.014	8:08	04.147
112.619	08.769	6:55	13.284	10:28	09.036		
112.785	08.935	9:12	13.379	11:06	09.062	Jan. 3, 6:06	06.062
113.647	09.797					7:09	06.106
		Nov. 29, 6:45	14.277	Dec. 9, 11:08	10.063	8:37	06.167
114.769	10.919	7:55	14.326	12:01	10.101		
121.680	03.433	9:10	14.378			Jan. 4, 7:38	07.126
124.689	06.442			Dec. 24, 10:38	10.647	8:25	07.159
126.667	08.420	Nov. 30, 6:05	00.853	11:10	10.669	9:15	07.193
130.640	12.393	7:17	00.903				
		8:26	00.951	Dec. 26, 10:17	12.632	Jan. 5, 9:38	08.209
130.780	12.533			11:17	12.674	10:35	18.249
132.635	14.388	Dec. 1, 6:57	01.890				
132.808	00.165	8:07	01.938	Dec. 27, 6:53	13.491	Jan. 6, 9:21	09.198
133.633	00.990	9:19	01.988	7:52	13.532	10:21	09.239
136.697	04.054	11:58	02.099	8:57	13.577	11:26	09.284
137.667	05.024	Dec. 2, 8:23	02.949	Dec. 28, 7:59	00.141	Jan. 7, 8:03	10.143
145.661	13.018	9:27	02.994	8:56	00.180	9:20	10.197
148.670	01.631			9:52	00.219	10:58	10.265
149.664	02.625	Dec. 4, 9:25	04.992				
150.658	03.619	10:32	05.039				

tions in the light of the star. HD 47129 is included in various cataolgues of O and B stars (Petrie 1950; Morgan, Whitford, and Code 1953, 1955; Hiltner 1956; Slettebak 1956). It is a probable member of the I Mon association connected with NGC 2244.

The New Observations and Orbit

This work is based on 25 Mills plates obtained by the author at the Lick Observatory and 20 Mount Wilson coudé plates obtained with the 100-inch telescope by Struve and Sahade. Table 6 gives the list of lines measured; all lines were given equal weight. The letters "Cd" and "LS" indicate that the line was measured on Mount Wilson or Lick plates, respectively. The measured radial velocities are assembled in Table 7*a*.

a) *Correction to the period.*—Plaskett's period for the binary produced a phase shift of −1.44 days in the velocity-curve for 1956–1957. Therefore, combining earlier observations by Plaskett and Struve, a definitive period of 14.3961 days was established (Abhyankar 1957). Consequently, phases of all available observations were computed from the expression

$$\text{Zero phase} = \text{JD } 2423031.870 + 14.3961E\,.$$

These are given in Tables 7*a* and 7*b*.

b) *The orbit.*—Two spectroscopic orbits were computed for the primary with the IBM 701 computer, one based on observations of 1956–1957 only and the other based on all available observations from 1922 to 1957. The orbits are given in the third and

TABLE 8

ORBITS OF HD 47129—PRIMARY

Elements and Units	Plaskett (1922)	Lick (1956–1957)	All Available Observations
γ_1 in km/sec	+ 23.94	+ 29.3 ± 1.0	+ 24.9 ± 0.8
K_1 in km/sec	206.4	203.9 ± 1.4	205.2 ± 1.0
Eccentricity e	0.035	0.024 ± .007	0.011 ± .005
ω in degrees	182.0	99.8 ±17.0	22.4 ±26.9
T_p: phase in days	.....	11.16 ± 0.68	8.07 ± 1.07
$a \sin i$ in 10^6 km	40.88	40.35	40.62
$f(\mathfrak{M})$ in solar masses	13.14	12.62	12.88

fourth columns of Table 8. There is no obvious change in the orbit between the first and the last epochs. Hence the orbit based on all observations is adopted as definitive. It was not possible to compute an orbit for the secondary because of scatter and the erratic nature of its behavior. Figure 4 represents all observations of the primary and the secondary.

The orbit of the primary is almost circular; therefore, the values of ω and T_p are not reliable. The mass function is large, but individual masses of the two components cannot be obtained because of uncertainty in the amplitude of the radial velocity-curve for the secondary. Assuming $\mathfrak{M}_1 = \mathfrak{M}_2$, we derive $\mathfrak{M}_1 \sin^3 i = \mathfrak{M}_2 \sin^3 i = 52$ solar masses, which are the smallest values obtainable from the assumption that the secondary is less massive than, or equal in mass to, the primary. With $\mathfrak{M}_2/\mathfrak{M}_1 = 0.8$, we obtain $\mathfrak{M}_1 \sin^3 i = 82\mathfrak{M}_\odot$ and $\mathfrak{M}_2 \sin^3 i = 65\mathfrak{M}_\odot$. Thus the mass of the system and the masses of each component are the largest known.

Figure 4 shows that the observed points for the primary lie very well on the computed curve. The secondary shows large scatter, a difference between γ_1 and γ_2, and a small value of K_2. We especially notice systematic differences from one epoch to another. For example, the McDonald observations in 1947 give $\gamma_2 = \gamma_1 - 100$ km/sec, while the

present data give a much smaller difference between γ_1 and γ_2; Plaskett's observations in 1922 lie somewhere in between. Also, the McDonald observations show a continuous increase in velocity from the conjunction at 10.8 days to the conjunction at 3.5 days; but the Lick observations show a curvature similar to that of the primary curve in this same interval. The points are much more uniformly scattered when the secondary has negative velocities, but the Lick observations give a smaller negative velocity, on the average, than the McDonald observations. If we assume that the erratic nature of the observations is due to gas streams, the systematic differences from one epoch to another indicate that the pattern of the gas streams also changes. Differences in the intensities of the secondary lines: strong in 1947 and weak in 1956–1957, which were observed by Struve (Struve, Sahade, and Huang 1958), also point to changes of this sort.

Quantitative Measurements of Line Intensities

The method described in Section IV was applied to obtain values of lk for various lines on five plates. Means of the results derived from equations (5*a*) and (5*b*) are assembled in Table 9.

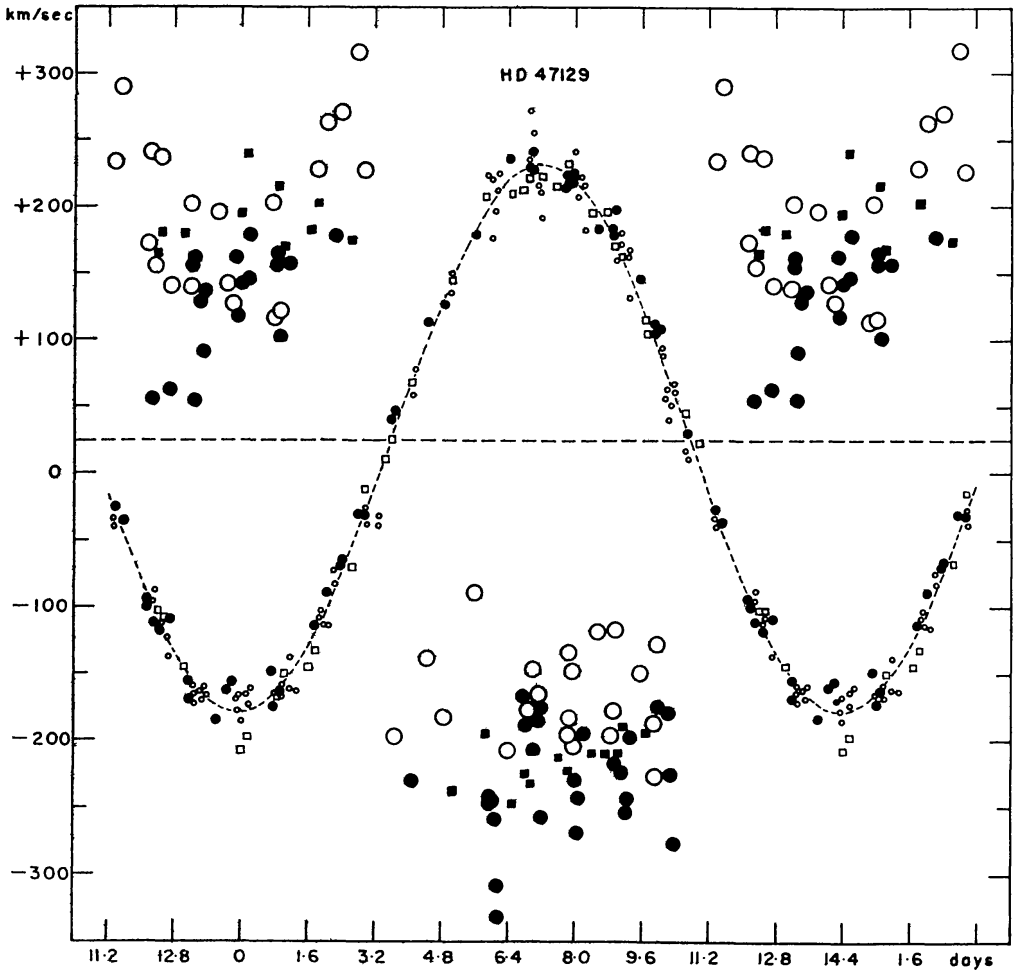

FIG. 4.—The radial velocity-curves for HD 47129

	Primary	Secondary
Victoria (1922)	Open squares	Filled squares
McDonald (1947–1948)	Small open circles	Large filled circles
Lick and Mount Wilson (1956–1957)	Small filled circles	Large open circles

1959ApJS....4..157A

Table 9

Measured values of ℓk for HD 47129

Region	Element or line	Date Phase in days	1957 April 12 9.900	1957 Jan. 18 12.309	1956 Nov. 22 13.202	1957 Mar. 21 2.364	Mean for four plates	1957 April 10 7.946	Factor giving increase in intensity at phase 7.95 days
Blue	H	No. of lines	3	6	4	5	18	6	
		Mean ℓk	.392	.437	.399	.400	.411	.525	1.3
	He I	No. of lines	6	4	2,	6	18	6	
		Mean ℓk	.258	.239	.302	.323	.279	.447	1.7
	He II	No. of lines	1	2	1	2	6	3	
		Mean ℓk	.268	.378	.389	.415	.377	.484	1.3
	All lines	No. of lines	10	12	7	13	42	15	
		Mean ℓk	.299	.361	.370	.370	.350 ± .030	.484 ± .017	1.4
		Δm					1.14 ± .09	0.79 ± .04	
Red	He I λ 5876	ℓk	---	.448	.294	.723	.488	.709	1.4
	λ 6678	ℓk	.950	----	----	----	.950	1.011	1.1
	Mean	ℓk					.719	.860	1.25
		Δm					0.36	0.14	

Table 10

'Normal' values of ℓ for various lines in HD 47129

Element	Line	Wave length	$1/\lambda$	ℓ	$-2.3 \log \ell$	No. of measures
H	Hγ	4340 A	2.304×10^{-4}	.305	1.186	2
	Hε	3970	2.519	.368	0.999	2
	Hζ	3889	2.571	.394	0.930	3
	H9	3835	2.608	.383	0.959	3
	H10	3798	2.633	.337	1.087	3
	H11	3771	2.652	.426	0.852	3
	H13	3734	2.678	.432	0.838	4
	Mean		2.566		0.979	
He I	$2^3P^o - 3^3D$	5876	1.702	.488	0.717	3
	- 4	4471	2.237	.240	1.426	3
	- 5	4026	2.484	.248	1.393	4
	- 6	3819	2.618	.237	1.438	2
	- 7	3705	2.699	.276	1.286	3
	- 9	3587	2.787	.402	0.910	1
	$2^1P^o - 3^1D$	6678	1.449	.950	0.051	2
	- 5	4388	2.279	.219	1.517	1
	- 6	4144	2.413	.344	1.066	3
	- 8	3926	2.547	.418	0.871	1
	Mean					
	Blue		2.508		1.238	
	Red		1.576		0.384	
He II	$4^2F^o - 9^2G$	4542	2.202	.425	0.855	4
	-10	3923	2.549	.566	0.569	1
	-11	3858	2.592	.305	1.186	2
	Mean		2.448		0.870	
Mean blue (all lines)			2.520		1.076	
Mean red (2 He I lines)			1.576		0.384	

1959ApJS....4..157A

Table 11

Differences : Velocity of H line - Mean velocity from all lines.

Mean phase in days	Hα v - $\bar{v}$ km/sec.	Hα No. of plates	Hβ v - $\bar{v}$ km/sec.	Hβ No. of plates	Hγ v - $\bar{v}$ km/sec.	Hγ No. of plates	(H9 + H10)/2 v - $\bar{v}$ km/sec.	(H9 + H10)/2 No. of plates
00.67	-----	---	-----	---	------	---	+ 20.3	5
00.73	-----	---	-----	---	- 06.8	8	------	---
01.99	-----	---	-----	---	+ 07.1	9	- 10.8	7
02.36	+ 147	1	-----	---	------	---	------	---
02.99	+ 129	2	-----	---	------	---	------	---
03.01	-----	---	-----	---	- 02.8	8	- 03.4	6
04.13	-----	---	-----	---	------	---	- 25.8	2
04.17	-----	---	-----	---	+ 02.0	4	------	---
05.39	-----	---	-----	---	- 36.0	6	------	---
05.48	-----	---	-----	---	------	---	- 16.2	4
06.70	-----	---	-----	---	- 66.4	10	- 14.8	9
06.94	- 243	1	- 109	2	------	---	------	---
07.90	- 266	2	- 104	4	------	---	------	---
07.95	-----	---	-----	---	- 70.9	9	- 14.8	8
08.92	- 122	2	-----	---	------	---	------	---
09.06	-----	---	-----	---	- 52.7	9	- 11.8	6
09.89	- 052	2	-----	---	------	---	------	---
10.24	-----	---	-----	---	- 40.4	12	- 09.2	10
11.40	- 101	2	-----	---	- 19.0	3	+ 06.0	4
12.39	- 087	3	-----	---	------	---	------	---
12.43	-----	---	-----	---	- 23.7	10	+ 05.6	8
12.50	-----	---	- 021	1	------	---	------	---
13.20	- 078	1	-----	---	------	---	------	---
13.74	-----	---	-----	---	- 20.9	13	- 01.8	9

a) *Blue lines.*—In the blue region there is good agreement in values of *lk* for the four plates with phases 9.9, 12.3, 13.2, and 2.4 days; their means in the seventh column of Table 9 give normal values of *lk*. Since both H and He II are relatively stronger than He I in the secondary spectrum, there is not much difference between the spectral types of the two components. Probably emission in the H and He II lines has reduced the strengths of these lines in the primary spectrum. Then, assuming $k = 1$, we obtain mean l in the blue region: $l = 0.35 \pm 0.03$ or $\Delta m = 1.14 \pm 0.09$.

At phase 7.95 days, *lk* is consistently greater by about 30–40 per cent for all three atoms H, He I, and He II. Probably absorption by additional numbers of atoms outside the secondary star has increased the depth, *k*, of the secondary lines at this phase. For this last plate, $lk = 0.48 \pm 0.02$, which corresponds to an apparent $\Delta m = 0.79 \pm 0.04$. Petrie (1950) had obtained similar values; since it seems unlikely that his plates had all phases around 7.2 days, the secondary lines were then probably relatively stronger than now, a conclusion in agreement with Struve's observations of 1947 and those of 1956–

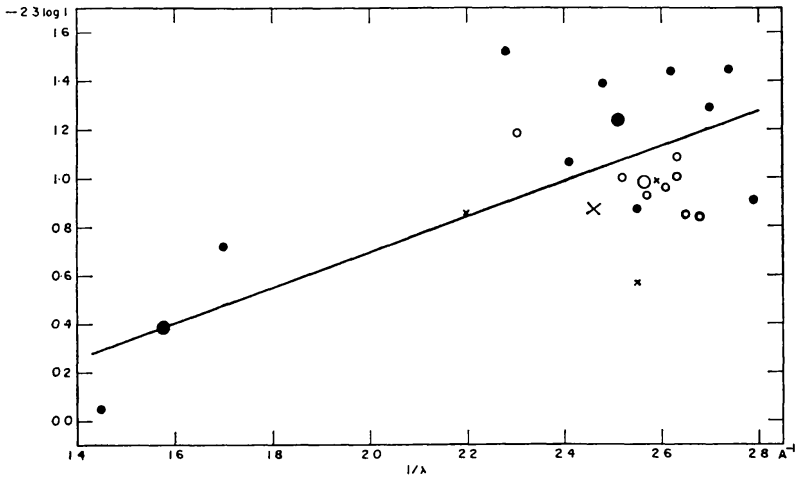

FIG. 5.—The relative spectrophotometric gradiant for the components of HD 47129. Filled circles represent He I lines; open circles and crosses represent H and He II lines, respectively. The larger symbols are the means. The numbers on the abscissa should be multiplied by 10^{-4}.

1957. Again we infer a change in the pattern of gaseous material in the system.

b) *Red lines.*—An increase in strength at phase 7.95 days is also shown by the red lines of He I, λ 5876 and λ 6678, although the strengthening is somewhat smaller. But the striking result is the large values of l that show a tendency to increase with wave length. Table 10 gives the normal values of l for all lines used in this study, and in Figure 5 the quantity $-2.3 \log l$ is plotted against $1/\lambda$. The best straight line drawn through all points has a slope equal to the relative spectrophotometric gradient for the two stars: $G_{AB} = 0.73 \times 10^4$. Since the temperature of the primary is about 30000°–35000°, we find for the secondary a temperature of about 10000°–11000°. This result is very puzzling, because there is no difference in the spectral types of the two components: we are concerned either with the presence of high-temperature lines in a cool star or with extinction of blue light from a hot star. In either case no simple explanation is apparent. If we assume that the secondary is a B-type star surrounded by an envelope that is heated by the ultraviolet radiation from the primary, the presence of the high-temperature lines in its spectrum may not be very hard to explain. But, even then, the relative strength of the red He lines will have to be accounted for.

Velocities of Hydrogen Lines

The effect of gaseous material on the primary spectrum is noticed in the velocities of the H lines at phases around 7.2 days. Table 11 gives the normal values of the difference:

the velocity of the H line *minus* the mean velocity from all lines; only the unblended lines are listed. The results plotted in Figure 6 show that all hydrogen lines have negative velocities with respect to the mean at phases when the primary is receding. They also look broad and fuzzy at the same phases. Struve, Sahade, and Huang (1958) had found evidence for flow of material from the secondary to the primary through the first Lagrangian point, L_1. According to recent extensive calculations by Gould (unpublished), this material will collect on the receding side of the primary. If it is now acted upon by the pressure of radiation from the primary, it will start moving outward and thus give rise to fuzzy lines with negative velocities. The material probably accelerates as it goes outward and causes shell lines with high negative velocities when the distance from the star is great enough to produce dilution effects. These shell lines will be discussed in the next section. The variation in the velocity of the lines of He I reported earlier (Abhyankar 1957) was spurious.

Figure 6 also shows that the difference in velocity is largest for Hα and becomes smaller as we go to higher members of the Balmer series. This is probably the effect of

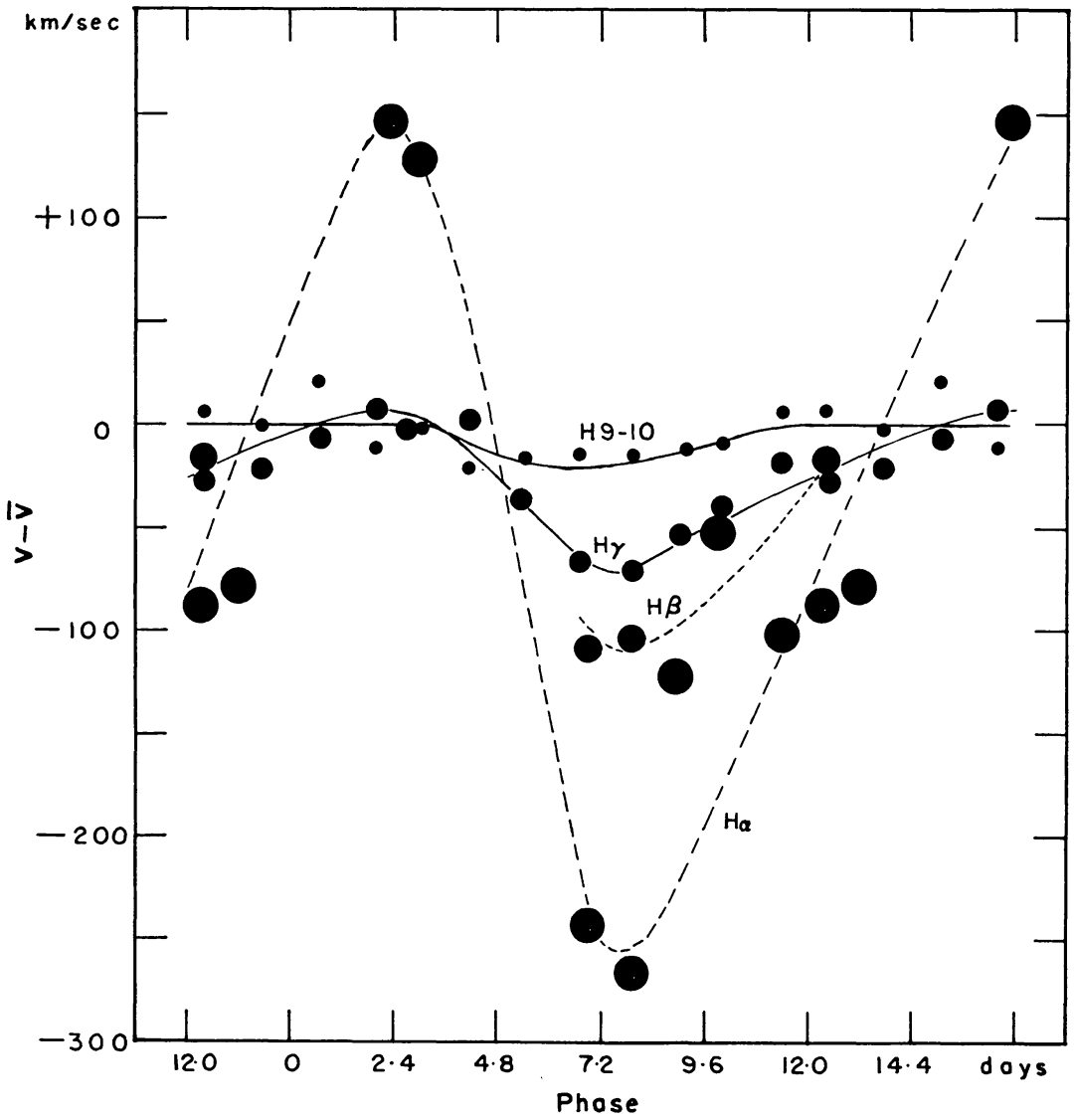

FIG. 6.—Velocities of hydrogen lines in the primary spectrum of HD 47129. Measures for Hα are taken from the work of Struve, Sahade, and Huang (1958).

emission, which is strongest in Hα and becomes rapidly weaker in the higher members of the series.

VI. THE STUDY OF SHELL LINES

Geometrical Dilution

The shell lines appear between phases 3.5 and 10.5 days, i.e., when the primary is receding. Only four lines of He I are seen: λλ 5876, 4471, and 4026 arising from the 2^3P° level and λ 3889 arising from the 2^3S level. The three triplet P lines can be used to determine the portion of the curve of growth on which the lines fall, and the relative strength of the triplet S line can then give the geometrical dilution factor. Table 12 gives the equivalent widths of the four lines on five nights when the lines were observed. It was assumed that the lines were produced in the material projected against the primary; the effect of the continuous spectrum of the secondary was removed by means of equation

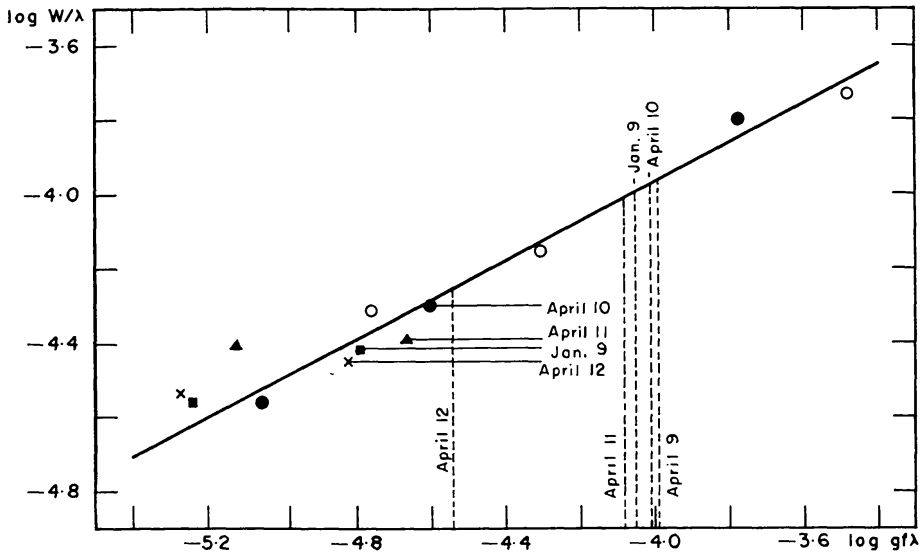

FIG. 7.—Curve of growth for shell lines of HD 47129

(4*a*), in which the observed variation of l with wave length was taken into account. The progressive weakening of all lines on the four nights which follow each other indicates differences in the density of material in various directions and probably also from cycle to cycle.

In Figure 7, the log W/λ's for the three triplet P lines are plotted against theoretical values of log $gf\lambda$, which were taken from the work by Trefftz, Schülter, Dettmar, and Jörgens (1957). The points for April 9 were fixed, and those for April 10 were shifted horizontally until a good fit was obtained. A straight line through the six points gives the portion of the curve of growth. The rest of the nights had only two measurable lines, which were used for determining only the shift along the horizontal co-ordinate; here the weak line λ 4026 was given half-weight. The seventh row of Table 12 contains the values of $\Delta \log N_{2^3P^\circ}$, corresponding to the horizontal shifts for each night. The envelope is almost three times thicker at phase 6.9 days (April 9) than at phase 9.9 days (April 12); the thickness on January 9 (3.6 days) is about the same as that on April 12.

Using the measured equivalent widths of λ 3889, if we read off the corresponding values of log $gf\lambda$ from the curve of growth and correct them for the difference in abundances for the night concerned, we obtain the values of $(\log gf\lambda_{3889})_{obs}$, which are given in the eighth row of Table 12. Subtracting $(\log gf\lambda_{3889})_{theor}$, we obtain the numbers

1959ApJS....4..157A

Table 12

Study of shell lines in Plaskett's star

1.	Date	1957	April 9	April 10	April 11	April 12	January 9
2.	Phase in days		6.9	7.9	8.9	9.9	3.6
	Equivalent widths W in milliangstroms.						
3.	$2^3P^o - 3^3D$	5876 A	1097	928	---	---	---
4.	- 4	4471	314	226	182	159	172
5.	- 5	4026	198	111	158	117	111
6.	$2^3S - 3^3P^o$	3889	425	412	383	218	393
7.	$\Delta \log N_{2^3P^o}$		0.000	- 0.294	- 0.360	- 0.512	- 0.480
8.	$(\log gf\lambda_{3889})_{obs}$		- 3.990	- 3.718	- 3.720	- 4.030	- 3.572
9.	$(\log gf\lambda_{3889})_{obs} - (\log gf\lambda_{3889})_{theor}$		1.240	1.512	1.510	1.200	1.658
10.	Geometrical dilution factor for T_s = 35000 degrees		.0160	.0094	.0094	.0181	.0064
11.	$(r/R)_{eff}$		4.0	5.2	5.2	3.8	6.2
12.	θ in degrees		97.5	72.5	47.5	22.5	180
13.	Secondary a cool star : (r_1/R_1)		4.0	5.2	5.2	3.8	6.2
14.	Secondary ≡ Primary : (r_1/R_1)		4.2	6.2	7.7	8.8	6.8
	(r_2/R_2)		10.4	9.2	7.0	4.9	15.8

given in the ninth row, which represent log ($N_{2^3S}/N_{2^3P^\circ}$) for each night. In the presence of dilution the normal Boltzmann equation is modified into

$$\frac{N_{2^3S}}{N_{2^3P^\circ}} = \frac{b_{2^3S}}{b_{2^3P^\circ}} \cdot e^{\chi_{SP}/kT_e}, \tag{6}$$

where the b's are functions of the dilution factor, $\mathfrak{W}$; the temperature of the star, T_s; and the electron temperature of the envelope, T_e. For any assumed values of T_s and T_e we obtain $b_{2^3S}/b_{2^3P^\circ}$ from equation (6) and then derive $\mathfrak{W}$ from Wellmann's (1952) tables of b-factors. It turns out that, for reasonable values of T_e (between 10000° and 50000°), $\mathfrak{W}$ is rather independent of T_e; but it depends strongly on T_e. For a stellar temperature of 35000° we obtain the dilution factors given in the tenth row of Table 12. The corresponding values of $(r/R)_{\text{eff}}$, where r is the mean distance of the envelope from the star and R is the radius of the star, are given in the eleventh row. The subscript "effective" is used to indicate that the observed dilution is the effect of the radiation from the two components of the binary.

Mean Distance of the Envelope

In order to take into account the effect of the secondary, we can make use of two equations: one geometrical, the other physical. Let r_0 be the distance between the two stars and r_1 and r_2 the mean distances from the two components of the region in the shell which is responsible for producing the shell lines at a certain phase. Let θ be the angle between the line joining the centers of the two stars and the line of sight. Then

$$r_2^2 = r_0^2 + r_1^2 - 2 r_0 r_1 \cos\theta . \tag{7}$$

Further, if R_1 and R_2 are the radii of the two components and T_1 and T_2 are their temperatures, we can write the plausible relation,

$$\left[\frac{R}{r}\right]^2_{\text{eff}} = \left[\frac{R_1^2}{r_1^2}\right] + \frac{F(T_2, \lambda)}{F(T_1, \lambda)}\left[\frac{R_2^2}{r_2^2}\right], \tag{8}$$

where $F(T, \lambda)$ is the Planck function for temperature T and wave length λ. Since the lower levels of the lines are metastable, they are reached from higher levels or from the continuum; therefore, the wave lengths concerned are shortward of 500–600 A.

If r_0, θ, R_1, R_2, T_1, and T_2 are known, we can compute r_1 and r_2 from equations (7) and (8). The greatest uncertainty is that of T_2; two limiting cases are considered, in both cases r_0 and R_1 were taken equal to 9×10^7 km and 10^7 km, respectively. The quantity θ for each night is given in the twelfth row of Table 12.

Case I.—If the secondary is really a cool star with a temperature of about 10000°, then F_2/F_1 will be a negligible fraction. Therefore, the secondary has no effect, and $(r/R)_{\text{eff}}$ will be equal to r_1/R_1. In this case the mean value of r_1/R_1 is about 4.9.

Case II.—If the secondary is identical with the primary, F_2 is equal to F_1, and R_2 is equal to R_1. Values of r_1/R_1 and r_2/R_2 for this case are given in the last row of Table 12. The mean value of r_1/R_1 is now about 6.7, and we notice a motion away from the primary with an average velocity of about 180 km/sec.

The actual situation lies somewhere in between, so that the mean distance of the envelope from the center of the primary is about six times the radius of the star. The velocity of expansion derived in case II is too small compared to the observed velocity of the shell with respect to the primary, viz., −900 km/sec. Therefore, the structure and the density of the shell vary in different directions and probably in different cycles. These changes might be connected with the irregular variations in the brightness of this star observed by Abhyankar and Spinrad (1958).

Physical Conditions in the Shell

On account of the small number of available points, the curve of growth for the shell was represented by a straight line; actually, it corresponds to the transition between the linear and the flat portions of the complete curve. On making the best fit with the theoretical curve of growth for an absorption tube (Unsöld 1955, p. 292), we obtain a vertical shift that gives the kinetic temperature of 24000°. Since the stellar temperature is about 35000°, the derived electron temperature of the shell is reasonable. Then the horizontal shift gives $N_{2^3P^0}\mathrm{H} = 2 \times 10^{13}$, and, for a dilution factor of 0.01, $T_e = 24000°$, the total number of neutral helium atoms in a column of 1 square centimeter cross-section turns out to be 10^{16}. Since the height of the shell is about $5R_1$, i e., 5×10^7 km, the number density of neutral helium atoms is $N_{\mathrm{He\,I}} = 2 \times 10^3$ atoms/cm^3.

Neglecting any continuous absorption in the shell, the ionization equation in the field of diluted radiation has the following form:

$$\frac{n_e n_i}{n_0} = \left[\frac{2\pi m k T_s}{h^2}\right]^{3/2} \frac{2g_i}{g_0}\, e^{-\chi/kT_s} \left(\frac{T_e}{T_s}\right)^{1/2} \mathfrak{W} = \phi\,.$$

Therefore, for hydrogen and helium we have,

$$\frac{n_e N_{\mathrm{H\,II}}}{N_{\mathrm{H\,I}}} = \phi_{\mathrm{H\,I}}\,, \tag{9a}$$

$$\frac{n_e N_{\mathrm{He\,II}}}{N_{\mathrm{He\,I}}} = \phi_{\mathrm{He\,I}}\,, \tag{9b}$$

$$\frac{n_e N_{\mathrm{He\,III}}}{N_{\mathrm{He\,II}}} = \phi_{\mathrm{He\,II}}\,, \tag{9c}$$

with

$$n_e = N_{\mathrm{H\,II}} + N_{\mathrm{He\,I}} + 2N_{\mathrm{He\,II}}\,. \tag{10}$$

Further, anticipating the results of Section VII, we write

$$\frac{N_{\mathrm{He}}}{N_{\mathrm{H}}} = \frac{N_{\mathrm{He\,I}} + N_{\mathrm{He\,II}} + N_{\mathrm{He\,III}}}{N_{\mathrm{H\,I}} + N_{\mathrm{H\,II}}} = 0.14\,. \tag{11}$$

As $N_{\mathrm{He\,I}}$ is known, equations (9*a*), (9*b*), (9*c*), (10), and (11) can be solved for the remaining five unknowns $N_{\mathrm{He\,II}}$, $N_{\mathrm{He\,III}}$, $N_{\mathrm{H\,I}}$, $N_{\mathrm{H\,II}}$ and n_e. By trial and error the following solution was obtained:

$$N_{\mathrm{H}} = 1.3 \times 10^{11}/\mathrm{cm}^3\,, \qquad N_{\mathrm{He}} = 0.2 \times 10^{11}/\mathrm{cm}^3\,, \qquad n_e = 1.7 \times 10^{11}/\mathrm{cm}^3\,;$$

$$\frac{N_{\mathrm{H\,I}}}{N_{\mathrm{H}}} = 1.25 \times 10^{-7}\,, \qquad \frac{N_{\mathrm{He\,I}}}{N_{\mathrm{He}}} = 1.19 \times 10^{-7}\,,$$

$$\frac{N_{\mathrm{He\,II}}}{N_{\mathrm{He}}} = 0.095\,, \qquad \frac{N_{\mathrm{He\,III}}}{N_{\mathrm{He}}} = 0.905\,.$$

The corresponding mean density in the shell is found to be 3.3×10^{-13} gm/cm^3. These values merge very well with the model of an O star computed by Underhill (1951*a*). With $T_e = 15000°$ the degree of ionization is reduced, and the densities are increased, by one order of magnitude; also we shall get a velocity of turbulence equal to about 20 km/sec.

If the envelope is a sphere of radius of $6R_1$, the total mass will be 2.5×10^{26} gm, which is about 10^{-9} times the mass of the system. Finally, the mean free path of about 1 km is

various orders of magnitude smaller than the thickness of the shell. Therefore, the flow of material in the shell would be governed by hydrodynamic equations in addition to the forces of gravitation.

VII. HE/H ABUNDANCE RATIO

Unsöld's (1941) classical method for τ Sco was employed to make a "Grob-Analyse" of the atmosphere of the primary star. Equivalent widths of H, He I, and He II lines were obtained from line profiles on five plates with double-line phases and one plate with single lines. The true equivalent widths of the lines were obtained by means of equations (4*a*) and (2*b*), in which l was taken equal to 0.35 and k was put equal to unity. The logarithms of the means of the six measures are given in the fourth column of Table 13. The accuracy for strong lines is about 10 per cent, and that for the weakest lines is about 20–30 per cent. The values of NH for the lower state obtained from the linear relation between equivalent width, W, and $\lambda^2 N\mathrm{H}f$, are given in the last column but one. They were reduced to a common geometrical depth in the atmosphere of the star, corresponding to an optical depth of about $\frac{2}{3}$ for λ 4100 or $\bar{\tau} = 0.25$. The required variation of τ with λ was taken from the model of 10 Lac worked out by Traving (1957); as the corrections are small, the actual model used is not of great consequence. In the case of He I, $N_{2^3\mathrm{P}^\circ}$ H was obtained in each case by applying a Boltzmann correction appropriate for a temperature of 35000°. The numbers in the last column include these corrections. They are plotted against n, the principal quantum number of the upper level, in Figure 8. The actual number of absorbing atoms is obtained asymptotically. The results are as follows:

$$\left.\begin{array}{lll} \text{Hydrogen, Balmer series,} & \log N_{02}\mathrm{H}, & 15.28\,, \\ \text{He II, Pickering series,} & \log N_{14}\mathrm{H}, & 15.12, \\ \text{He I, } 2^1\mathrm{P}^\circ - \mathrm{n}^1\mathrm{D} \text{ series,} & \log N_{2^3\mathrm{P}^\circ}\mathrm{H}, & 14.85, \\ 2^1\mathrm{P}^\circ - \mathrm{n}^1\mathrm{D} \text{ series,} & \log N_{2^3\mathrm{P}^\circ}\mathrm{H}, & 14.49, \\ 2^3\mathrm{P}^\circ - \mathrm{n}^3\mathrm{S} \text{ series,} & \log N_{2^3\mathrm{P}^\circ}\mathrm{H}, & 15.21, \\ 2^3\mathrm{P}^\circ - \mathrm{n}^3\mathrm{D} \text{ series,} & \log N_{2^3\mathrm{P}^\circ}\mathrm{H}, & 14.88, \\ \text{Mean} & \log N_{2^3\mathrm{P}^\circ}\mathrm{H}, & 14.86 \pm 0.20 \end{array}\right\} \quad (12)$$

Electron Pressure

i) *Hydrogen.*—Fifteen lines of the Balmer series are seen on the microphotometer tracings. Therefore, from the Inglis-Teller formula we obtain $\log N_e = 14.44$. Further, the equivalent width of the Stark-broadened Hγ line is given by,

$$W(A) = 7.63 \times 10^{-6} \Re_c^{3/5} (N_{02}\mathrm{H} \cdot N_e k)^{2/5} \quad (13)$$

(Unsöld 1955, p. 478). On correcting the central depth of the Hγ line for the effect of the secondary by equations (2*a*) and (3*a*) and for the rotational broadening of 120 km/sec (Slettebak 1956), the true value of $\Re_c$ is found to be 0.36. Then, putting $\log W = 1.566$ and $\log N_{02}\mathrm{H} = 15.28$ in equation (13), we derive $\log N_e = 14.53$. The mean of the two values is $\log N_e = 14.48$, which is the electron density at the optical depth, τ_{H}, where the hydrogen lines are produced.

ii) *Helium.*—It is easy to show that for He II the modified form of the Inglis-Teller formula is

$$\log N_e = 24.61 - 7.5 \log n_m\,.$$

Therefore, putting $n_m = 20$, we get $\log N_e = 14.86$. Finally, applying the combined Saha-Boltzmann formula to populations of N_{14} and $N_{2^3\mathrm{P}^\circ}$ levels of He II and He I, re-

Table 13

Equivalent widths of H and He lines in HD 47129 - primary.

Element and line.		Wave length in A	f*	log W(mA)	log NH lower state	log NH at τ ~ .25	
H	Hγ	4340	4.47×10^{-2}	3.195	14.322	14.36	N_{02}
	Hδ	4102	2.21 "	---	----	---	
	Hε	3970	1.27 "	3.085	14.836	14.81	
	H 8	3889	8.04×10^{-3}	---	----	---	
	H 9	3835	5.43 "	3.080	15.230	15.18	
	H10	3798	3.85 "	2.993	15.280	15.23	
	H11	3771	2.84 "	2.880	15.328	15.27	
	H12	3750	2.15 "	2.743	15.316	15.25	
	H13	3734	1.67 "	2.627	15.313	15.25	
	H14	3722	1.33 "	2.516	15.303	15.23	
	H15	3712	1.07 "	2.366	15.250	15.18	
	H16	3704	8.77×10^{-4}	2.164	15.136	15.06	
He II 4^2F^o	- 9^2G	4542	1.86×10^{-2}	2.880	14.349	14.42	N_{14}
	- 15	3923	2.06×10^{-3}	2.501	15.002	14.97	
	- 17	3858	1.44 "	2.430	15.153	15.11	
	- 19	3814	1.01 "	2.288	15.175	15.12	
	- 21	3782	7.5×10^{-4}	2.041	15.063	15.00	
He I 2^3P^o	- 4^3S	4713	1.16×10^{-2}	2.605	14.248	14.32	N_{23P^o}
	- 5	4121	4.27×10^{-3}	2.328	14.521	14.52	
	- 6	3868	2.09 "	2.265	14.822	14.78	
	- 7	3733	1.17 "	2.240	15.084	15.02	
	- 8	3652	7.08×10^{-4}	2.210	15.289	15.21	
2^3P^o	- 4^3D	4472	1.23×10^{-1}	2.942	13.605	13.67	
	- 5	4026	4.67×10^{-2}	2.942	14.116	14.10	
	- 6	3820	2.31 "	2.773	14.298	14.25	
	- 7	3705	1.34 "	2.704	14.531	14.46	
	- 8	3634	8.49×10^{-3}	2.675	14.679	14.86	
	- 9	3587	5.78 "	2.529	14.710	14.87	
	- 10	3554	4.07 "	2.314	14.655	14.81	
2^1P^o	- 5^1S	4438	3.16×10^{-3}	2.170	14.430	14.53	
	- 6	4169	1.51 "	2.170	14.803	14.85	
2^1P^o	- 5^1D	4388	4.30×10^{-2}	2.576	13.711	13.80	
	- 6	4144	2.10 "	2.554	14.051	14.10	
	- 7	4009	1.19 "	2.456	14.228	14.25	
	- 8	3927	7.41×10^{-3}	2.389	14.384	14.39	
	- 9	3872	5.00 "	2.255	14.433	14.43	
	- 10	3834	3.51 "	---	----	---	
	- 11	3806	(2.54) "	2.021	14.507	14.49	

* Oscillator strengths of He I lines were taken from the paper by Trefftz et al., quoted earlier in the text. The f-value for λ3806 given in parenthesis is interpolated. For the 'Brackett' series of He II the asymptotic formula $6.95/n^3$ was used for n≥15. The f-value for λ4541 was taken from the work of Underhill (1951).

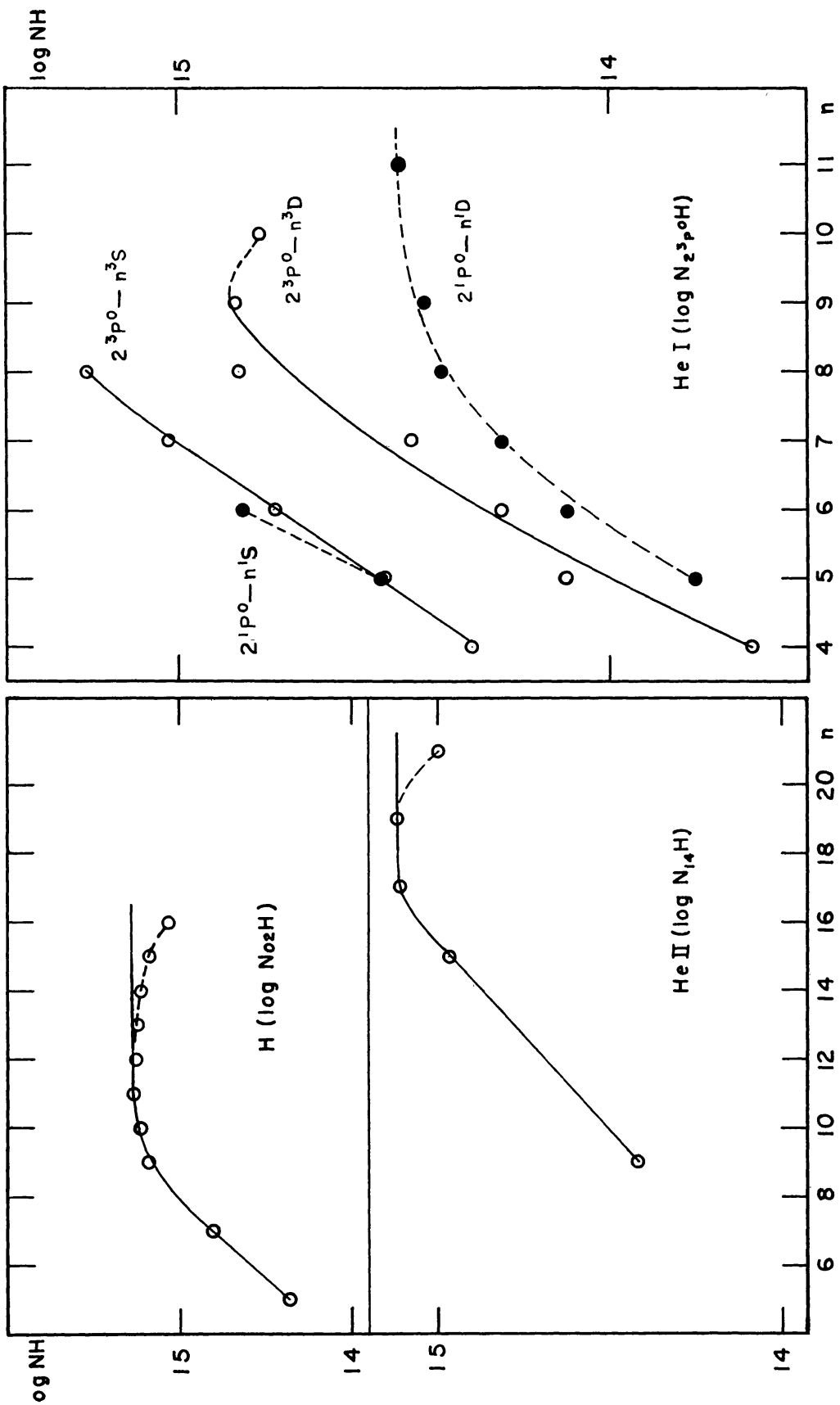

FIG. 8.—Abundance of H, He II, and He I atoms in HD 47129

spectively, we obtain log $N_e = 14.88$ with a temperature of 35000°. Then the electron density at the optical depth τ_{He}, where the helium lines are produced, is log $N_e = 14.87$, or

$$(\log N_e)_{\tau_{He}} - (\log N_e)_{\tau_H} = 0.39 \pm 0.05 . \tag{14}$$

Since the helium lines are produced deeper in the atmosphere than the hydrogen lines, the difference in the electron densities is in the right direction. The temperature at τ_{He} will also be higher than the temperature at τ_H. All these differences have to be taken into account in comparing the abundances of H and He.

Abundance of He

Because of the high temperature, most of the hydrogen is ionized, and most of the helium is singly and doubly ionized. Therefore, $N_H H = N_{H\,II} H$, and $N_{He} H = N_{He\,II} H + N_{He\,III} H$. Also,

$$\left[\frac{N_{He}H}{N_H H}\right]_{\tau_H} = \frac{(N_{He}H)_{\tau_H}}{(N_{He}H)_{\tau_{He}}} \times \frac{(N_{He}H)_{\tau_{He}}}{(N_H H)_{\tau_H}} .$$

Then, from the Saha-Boltzmann formula, we obtain

$$\left[\frac{N_{He}H}{N_H H}\right]_{\tau_H} = \frac{(N_{He}H)_{\tau_H}}{(N_{He}H)_{\tau_{He}}} \frac{(N_e)_{\tau_H}}{(N_e)_{\tau_{He}}} \left(\frac{T_{\tau_{He}}}{T_{\tau_H}}\right)^{3/2} \times \left[\frac{2/9\,(N_{2^3P^\circ}H)_{\tau_{He}}\, e^{-3.61\,eV/kT_{\tau_{He}}} + 1/32\,(N_{He\,14}H)_{\tau_{He}}\, e^{-3.37\,eV/kT_{\tau_{He}}}}{1/8\,(N_{H02}H)_{\tau_H}\, e^{-3.39\,eV/kT_{\tau_H}}}\right] .$$

Since T_{τ_H} and $T_{\tau_{He}}$ are both of the order of 35000°, the exponential terms, when divided by $e^{-3.37\,eV/kT}$, will all be very nearly equal to unity. Therefore, the difference between T_{τ_H} and $T_{\tau_{He}}$ is not important in the exponential terms. Thus, putting $T = 35000°$, we have

$$\left[\frac{N_{He}H}{N_H H}\right]_{\tau_H} = \frac{(N_{He}H)_{\tau_H}}{(N_{He}H)_{\tau_{He}}} \frac{(N_e)_{\tau_H}}{(N_e)_{\tau_{He}}} \left(\frac{T_{\tau_{He}}}{T_{\tau_H}}\right)^{3/2} \times \left[\frac{0.205\,(N_{2^3P^\circ}H)_{\tau_{He}} + 1/32\,(N_{He\,14}H)_{\tau_{He}}}{0.126\,(N_{H02}H)_{\tau_H}}\right] . \tag{15}$$

Now $P_g(\tau) = g_{eff} m_H (N_H H + 4N_{He}H)_\tau = 2\,P_e(\tau)$ for a hot star, and $(N_{He}H/N_H H) =$ constant. Therefore, $(N_{He}H)_\tau \propto P_e(\tau) \propto N_e(\tau) T(\tau)$. Or

$$\frac{(N_{He}H)_{\tau_H}}{(N_{He}H)_{\tau_{He}}} = \frac{(N_e)_{\tau_H}}{(N_e)_{\tau_{He}}} \times \frac{T_{\tau_H}}{T_{\tau_{He}}} . \tag{16}$$

Substituting equations (16), (12), and (14) in equation (15), we obtain

$$\frac{N_{He}H}{N_H H} = (0.13 \pm 0.03) \left(\frac{T_{\tau_{He}}}{T_{\tau_H}}\right)^{1/2} . \tag{17}$$

Assuming a simple model: $T^4 = T_0^4 (1 + \frac{3}{2}\tau)$, the factor

$$\left(\frac{T_{\tau_{He}}}{T_{\tau_H}}\right)^{1/2} = \frac{1 + 3/16\,\tau_{He}}{1 + 3/16\,\tau_H} .$$

In Traving's model of 10 Lac, He I lines are produced at an optical depth of about 0.1 and the He II lines at a depth of about 0.27. The hydrogen lines are produced much higher in the atmosphere. Assuming a mean optical depth of 0.2 for He lines and neglect-

ing τ_H, we derive: He/H = 0.14 ± 0.03 by numbers. This represents a reasonable abundance of helium. However, it should be emphasized that the result depends quite critically on the derived difference in the electron densities at the optical depths where the H and He lines are produced.

VIII. DISTANCE OF HD 47129

The equivalent widths of interstellar D_1 and D_2 lines in the spectrum of the star are found to be 536 and 665 mA, respectively, with a ratio of 1.24. Interstellar H and K lines of Ca II have equivalent widths of 227 and 370 mA, respectively, with a ratio of 1.64. Then Münch's (1957) curve of growth gives 17.4×10^{12} Na I atoms and 5.75×10^{12} Ca II atoms in the line of sight. According to the work of Binnendijk (1952), these numbers correspond to distances of 1070 parsecs for Na I atoms, and 1000 parsecs for Ca II atoms, in the direction of Plaskett's star (galactic longitude 173°). Hiltner's (1956) photometric data and McCuskey's (1956) determination of the photographic extinction as a function of galactic longitude and distance from the sun give a distance of 1300 parsecs for HD 47129. Also the mean distance of the I Mon association, of which Plaskett's star is supposed to be a member, is 1.4 kpc. Therefore, the mean, 1140 parsecs, should be a good estimate for the distance of the star. Then, with Hiltner's data, we get true $m_V = 4.97$ and $M_V = -5.31$. Further, if the two components have the same visual magnitude, as indicated by the intensities of red lines, then each will have an absolute visual magnitude equal to −4.6, which is consistent with the spectral type O8.

IX. AO CASSIOPEIAE

Since the announcement of the binary nature of AO Cas (Boss 46) in the annual report of the Mount Wilson Observatory (1916, p. 270), this star (MK type O9 III) was observed and studied spectroscopically by Adams and Stromberg (1918), Pearce (1926), and Struve and Horak (1949); photometrically by Guthnick (1920), Stebbins (1928), Guthnick and Pavel (1922), Guthnick (1923*b*), Güssow (1929), Bennett (1938), Wood (1948), and Horak (1949); and spectrophotometrically by Dadaev (1954) in the continuous spectrum and by Petrie (1950) in the line spectrum. The computed spectroscopic orbits, which are given in Table 15, have small eccentricities; but the mass ratio is not uniquely determined. Photometric light-curves indicate principally an ellipsoidal variation with shallow partial eclipses. But the light-curve varies from one epoch to the next and shows varying amounts of asymmetry. Combining spectroscopic and photometric data, absolute dimensions of the system have been obtained by Pearce, Wood, and Dadaev; they obtain ellipsoidal stars that are almost in contact. The most interesting observation is the sudden change in the period, from 3.52341 to 3.52355 days, found by Wood (1949); even the new period does not seem to satisfy later observations by Hiltner and Dadaev.

Spectroscopic Observations and Results

The observational material for the present study consisted of 47 Lick plates and 17 coudé and 11 Cassegrain plates obtained at Mount Wilson. Table 6 contains the list of measured lines, and Table 14 gives the observed velocities for the two components. The orbit of the primary, calculated by the IBM 701 computer, is given in the last column of Table 15. The observations are represented by this orbit in Figure 9. Taking e, ω, and T_p from the primary orbit, two solutions were made for the secondary: one for $\gamma_2 = \gamma_1$ and the other for $\gamma_2 \neq \gamma_1$. For both solutions, K_2 and, consequently, $\mathfrak{M}_1/\mathfrak{M}_2$ are essentially the same. The following conclusions can be drawn from a comparison of the four orbits given in Table 15:

i) The last three orbits give almost the same values for γ_1 and e; therefore, their means, $\gamma_1 = -31.1 \pm 0.7$ km/sec and $r = 0.035 \pm 0.004$, should be quite definitive.

1959ApJS....4..157A

Table 14

Measured velocities of AO Cassiopeiae.

Date	Phase in days	v_1 km/sec.	v_2 km/sec.	Velocity of Ca II km/sec.
Lick plates:				
1956				
Aug. 11, 9:10 UT	3.284	- 030.9	-----	----
Aug. 24, 8:34	2.165	+ 157.6	- 163.6	----
11:37	2.292	+ 206.5	- 150.4	----
Aug. 31, 11:34	2.243	+ 182.8	- 151.3	----
Sep. 3, 7:30	1.549	- 038.8	-----	----
Sep. 4, 7:18	2.541	+ 156.8	- 147.6	----
Sep. 6, 11:21	1.183	- 187.4	+ 158.6	----
Sep. 9, 6:46	0.472	- 223.7	+ 115.5	----
Sep. 11, 7:18	2.494	+ 209.5	- 174.7	----
Sep. 12, 12:05	0.170	- 178.0	-----	----
Sep. 29, 10:15	3.000	+ 113.8	- 125.6	----
Sep. 30, 6:25	0.316	- 192.3	+ 110.7	----
9:37	0.450	- 223.6	+ 101.5	----
Oct. 20, 8:34	2.788	+ 165.7	- 154.3	----
Oct. 21, 4:27	0.093	- 142.8	+ 180.4	----
8:11	0.249	- 151.0	+ 119.0	----
Nov. 3, 7:49	2.663	+ 198.8	- 188.0	----
Nov. 4, 7:12	0.114	- 139.0	-----	----
Nov. 23, 3:13	1.330	- 132.0	+ 173.9	----
6:17	1.458	- 078.2	-----	----
Nov. 24, 3:13	2.330	+ 213.4	- 148.1	----
6:22	2.461	+ 167.6	- 159.2	----
Dec. 21, 3:56	1.171	- 202.3	+ 120.3	----
Dec. 23, 4:12	3.182	+ 026.6	-----	----
Dec. 24, 3:41	0.637	- 244.8	+ 124.1	----
Dec. 25, 3.58	1.649	- 033.6	-----	----
1957				
Sep. 9, 7:12	2.565	+ 192.4	- 170.2	----
11:03	2.725	+ 189.4	- 142.6	----
Sep. 11, 11:03	1.201	- 166.0	+ 196.8	----
Sep. 13, 10:45	3.189	+ 039.8	- 216.1	----
Sep. 21, 10:28	0.606	- 263.7	+ 135.2	----
Sep. 24, 6:16	3.431	- 054.9	-----	----
Sep. 25, 5:55	0.894	- 209.2	+ 121.2	----
Oct. 8, 5:08	3.290	000.0	- 200.2	----
Oct. 16, 5:07	0.719	- 258.4	+ 142.1	----
9:11	0.889	- 250.1	+ 108.4	----
Oct. 17, 4:51	1.708	- 036.6	-----	----
Oct. 31, 3:57	1.576	- 046.3	-----	----
7:48	1.736	- 016.2	-----	----
Nov. 26, 6:09	3.003	+ 141.8	- 138.4	----
Dec. 2, 5:35 UT	1.932	+ 073.5	- 211.8	----
Dec. 9, 5:07	1.865	+ 056.3	-----	----
Dec. 11, 4:53	0.332	- 173.7	+ 100.4	----
Dec. 12, 4:53	1.332	- 155.8	+ 232.7	----
Dec. 23, 4:20	1.739	- 012.1	-----	----
Dec. 25, 4:10	0.209	- 148.2	+ 136.2	----
1958				
Jan. 5, 3:49	0.623	- 242.6	+ 172.5	----
Mount Wilson 100 inch coudé plates:				
1957				
Sep. 11, 10:13	1.167	- 181.4	+ 164.7	- 18.60, -----
11:22	1.215	- 175.0	+ 140.6	- 17.51, -40.18
12:29	1.261	- 175.4	+ 154.2	- 16.03, -----
Sep. 13, 8:38	3.101	+ 086.5	- 184.8	- 16.34, -36.67
9:53	3.153	+ 096.5	- 162.6	- 19.53, -----
Sep. 14, 9:18	0.606	- 240.7	+ 124.2	- 15.52, -34.67
10:29	0.655	- 237.5	+ 124.6	- 15.22, -35.54
Oct. 2, 8:22	0.949	- 239.2	+ 116.3	- 13.22, -34.95
9:53	1.012	- 244.2	+ 104.1	- 18.63, -----
11:25	1.076	- 218.4	+ 086.6	- 15.24, -35.93
Oct. 3, 8:22	1.949	+ 064.9	-----	- 16.16, -----
Oct. 4, 8:12	2.942	+ 138.0	- 130.4	- 14.96, -37.18
9:38	3.001	+ 123.4	- 140.8	- 14.68, -31.08
10:56	3.056	+ 110.1	- 149.9	- 19.00, -----
Oct. 5, 8:04	0.412	- 210.3	+ 132.4	- 16.07, -35.20
9:18	0.464	- 211.9	+ 121.5	- 15.41, -----
11:06	0.538	- 228.0	+ 101.6	- 16.67, -36.18
Mount Wilson 60 inch cassegrain plates:				
1957				
Sep. 14, 9:42	0.622	- 242.9	+ 157.9	- 20.72
10:54	0.672	- 236.4	+ 183.4	- 23.99
12:16	0.729	- 254.8	+ 177.9	- 22.48
Sep. 15, 9:40	1.621	- 036.6	-----	- 19.43
11:10	1.683	- 022.6	-----	- 23.51
12:36	1.743	- 004.1	-----	- 20.40
Sep. 16, 9:33	2.616	+ 204.4	- 202.0	- 21.30
10:53	2.671	+ 185.6	- 173.4	- 28.54
12:20	2.732	+ 161.7	- 192.3	- 25.45
Sep. 18, 9:58	1.109	- 220.4	+ 157.7	- 26.69
11:36	1.177	- 204.7	+ 139.5	- 22.85

1959ApJS....4..157A

Table 15

Orbits of AO Cassiopeiae.

Element	Units	Adams and Stromberg 1916–17	Pearce 1926	Struve and Horak 1948–49	Abhyankar 1956–57
Epoch E	Cycles	- 3111	- 2324	+ 200	+ 1068
γ_1	km/sec.	- 44.9 ± 5.5	- 29.34 ± 1.09	- 32.9 ± 1.1	- 31.1 ± 1.3
K_1	"	217.4 ± 3.4	218.45 ± 1.81	236 ± 1.6	223.4 ± 1.8
e		0.094 ± .020	0.037 ± .007	0.030 ± .007	0.037 ± .008
ω	degrees	323.0 ± 10.2	210.16	335 ± 12.5	020.8 ± 13.3
T_p	JD 2400000 +	21231.365	24003.703	32898.224	35957.058 ± .130
T_{δ}	"		24005.151	32898.455	35956.869 ± .005
$a_1 \sin i$	10^6 km.	10.48	10.84	11.4	10.82
f(m)	solar massess	3.71	3.80	4.81	4.06
K_2	km/sec.	——	234.59 ± 2.11	170*	174.8 ± 6.2 for $\gamma_2 = \gamma_1$ **178.8 6.1 for $\gamma_2 \neq \gamma_1$
m_1/m_2		——	1.074	0.72	0.83 for $\gamma_2 = \gamma_1$ 0.85 for $\gamma_2 \neq \gamma_1$
n_1	No. of plates	34	46	183	75
ϱ_1	km/sec.	——	——	9.9	11.2
n_2	No. of plates	——	——	——	58
ϱ_2	km/sec.	——	——	——	38.5 for $\gamma_2 = \gamma_1$ 36.6 for $\gamma_2 \neq \gamma_1$

* See Dadaev (1954), p. 72.

** When $\gamma_2 \neq \gamma_1$, $\gamma_2 = -12.7 \pm 4.9$ km/sec.

The first orbit by Adams and Stromberg, which gives very different results, will be ignored.

ii) In Figure 10 the values of ω for the last three orbits are plotted against the number of cycles computed from the zero point and the period given by Wood. They lie remarkably well on a straight line. It is almost certain that we have discovered a rotation of the line of apsides, in spite of the small value of the eccentricity. The slightly different period used by Pearce will not change the value of ω, obtained by him, by more than $0^{\circ}.2$, although the phases at node and at periastron will be shifted relative to those of the latter two series of observations. The effect of apsidal motion on the position of the secondary minimum with respect to primary eclipse is obscured by extraneous effects upon the light-curve, which has quite shallow minima; ω is given by the expression

$$\omega = 326^{\circ}.3 \pm 0^{\circ}.7 + (0^{\circ}.0500 \pm 0^{\circ}.0005)E .$$

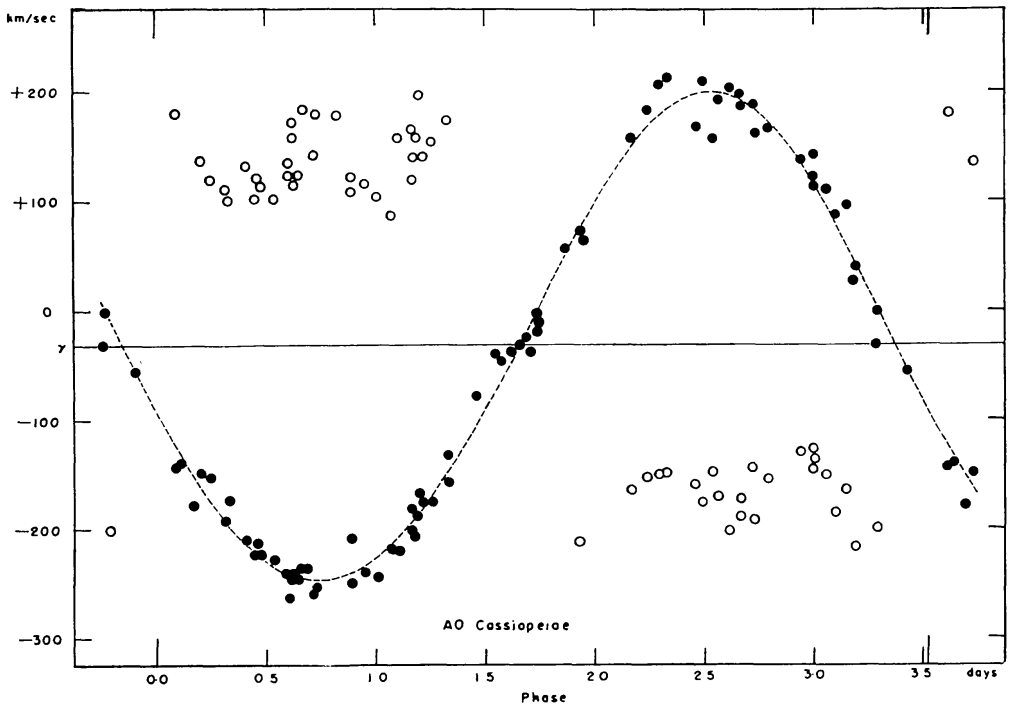

FIG. 9.—The radial velocity-curves for AO Cassiopeiae

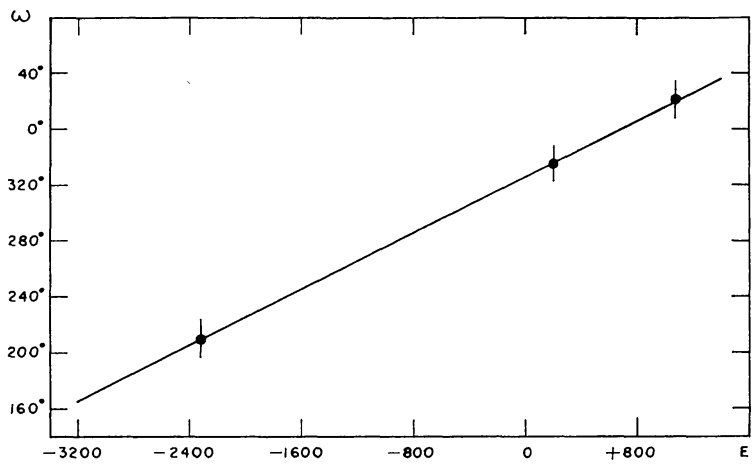

FIG. 10.—Apsidal motion in AO Cassiopeiae

It gives $U/P = 7200 \pm 70$, corresponding to a period of rotation of the line of apsides equal to 70 years. Substituting in equation (1) with Wood's values $R_1/r = 0.4$ and $R_2/r = 0.3$, we derive $k_1 = k_2 = 0.00065$, appropriate for a polytropic index slightly greater than 4. It is interesting to note that Russell (1939) had listed $k = 0.0006$, which, however, was based on more flimsy data.

iii) When equality of the γ's was not assumed, γ_2 was found to be 18.4 km/sec positive with respect to γ_1; the difference in the two γ's is smaller but similar to that of β Sco. This again raises the question of systematic errors of measurement of the secondary lines. In the present case ρ_2, the probable error of one plate, is only slightly improved by letting γ_2 differ from γ_1; moreover, the secondary measures plotted in Figure 9 do not show a curvature of the radial velocity-curve in the right direction, the points being widely scattered. Hence we believe that the difference in γ's found for AO Cas is only computational and may not be real. On the other hand, in the case of β Sco the plotted points show a definite curvature of the radial velocity-curve of the secondary in the expected direction; and the equalization of the γ's increased the probable error of one plate to two or three times its value when they were not equal, as the entries in Table 4 show. Therefore, for β Sco the difference in the γ's seems to be observationally established.

iv) The values of K_1 and the mass function obtained by Struve and Horak are somewhat larger than in the other three orbits, which are in good agreement. On the other hand, the orbits of 1956–1957 and 1948–1949 both have $K_2 < K_1$ and $\mathfrak{M}_1/\mathfrak{M}_2 \sim 0.8$; Pearce, in 1926, had obtained $\mathfrak{M}_1/\mathfrak{M}_2 = 1.07$. These observed changes of K_1, K_2, and the mass ratio certainly do not represent changes in the mass of the system or the distribution of mass among the two components. Are they possibly the effects of variable gas streams which might also affect the shape of the light-curve?

v) Petrie (1950) found that the secondary is 0.78 ± 0.05 mag. fainter than the primary, but spectroscopic orbits require that the secondary be comparable to, or larger than, the primary in mass. This contradiction of the mass-luminosity law can be removed if there is sufficient reflection to reduce the velocity amplitude of the secondary. But photometric observations give negative reflection effects. It appears that the secondary is underluminous.

Photometric Observations

Table 16 lists the dates of observations in the first column and gives the condition of the night and the epoch in periods based on Wood's expression in the next two columns. The serial numbers in the last column arrange the observations in order of increasing phase. Generally four, and sometimes three, consecutive points were averaged to obtain the normal points given in Table 17. The order of points was broken only for two nights, viz., September 7, 1957, and September 16, 1957, when AO Cas was fainter than a smooth curve would indicate; Figure 11 shows this quite clearly. Unfortunately, the check star BD+51°62 was not observed on these two nights. But, although the total range of the difference BD+51°62 − BD+47°50 from night to night was as great as 0.03 mag. in all three colors, observations of AO Cas lie very well on a smooth curve on all nights except the two mentioned above. We conclude that the observed deviations indicate irregular variations of about 0.03 mag. superposed on the smooth form of the light of AO Cas. In fact, such irregularities were mentioned by Wood (1948), as well as by Guthnick (1920).

The primary minimum occurred at phase 3.457 days, i.e., 353°.2 instead of zero phase; this is the value of θ_0 used in computing $\theta - \theta_0$ in Table 17. The amount of light, L, at normal phases is expressed in terms of the average of the lights at the two maxima, which differed by about 0.011 mag. in *Vl* and by about 0.02 mag. in *Bl* and *Ul*. The normal points are plotted in Figure 11.

Table 16

Dates of photometric observations of AO Cas.

Date	Condition of the night	E	Serial numbers of observations
1957			
Aug. 19, 7:21 to 10:57 UT	North wind.	1100	248 to 251, 253-54-56-58, 260 to 266.
Aug. 31, 7:08 to 11:43	Humid.	1104	58-60-62-64-66-68-70-71-73-75, 77 to 88.
Sep. 6, 4:41 to 8:09	Haze at the end.	1105	268 to 281, 283-84-86.
Sep. 7, 4:39 to 10:23	Good night.	1106	38-39-40, 42 to 57, 59-61-63-65-67-69, 72-74-76.
Sep. 10, 4:17 to 4:36	Poor seeing, clouds.	1106	305-06-08.
Sep. 15, 8:33 to 12:25	High humidity.	1108	174-76-78, 180 to 187, 189 to 191, 193-94-96-97-98.
Sep. 16, 5:33 to 10:53	High humidity, low fog.	1108	213 to 218, 220-22-26-28-30-33-34-36, 238 to 247.
Sep. 22, 4:16 to 6:19	Ultraviolet extinction large.	1110	153 to 159, 161-62-64-66.
Sep. 26, 4:15 to 4:54	Haze and clouds.	1111	200-01-02.
Oct. 2, 8:47 to 11:19	Very high humidity.	1113	105-07-11-14-16-18-21-24-29-33.
Oct. 4, 3:36 to 4:41 & 7:58	High humidity, fog.	1113	252-55-57-59-67.
Oct. 5, 3:29 to 9:38	High humidity.	1114	14-18, 21 to 37, 41.
Oct. 15, 7:10 to 10:56	Humid, low haze.	1116	295 to 304, 307-09-10-12.
Nov. 4, 3:03 to 7:14	Partly cloudy.	1122	203 to 212.
Nov. 9, 2:42 to 4:33 6:26 to 10:08	Fog and wind. Good night.	1123-24 1124	311-13-14-15, 1 to 3. 4 to 10, 12-15-17-19.
Nov. 10, 4:28 to 8:11	Partly cloudy at the end.	1124	119-26-28-31-35-37-38-41-43-45-49-50-52.
Nov. 21, 3:08 to 8:00	Strong North wind, haze.	1127	160-63-65, 167 to 171, 173-75-77-79.
Nov. 24, 3:20 to 9:41	Some haze at the start, became clearer and clearer.	1128	95-97-99, 102-04-08-10-12-17-20-23-30-34, 36-39-42-46.
Nov. 29, 6:26 to 8:47	Strong North-East wind.	1129	219-21-23-25-29-31-35-37.
Dec. 1, 2:45 to 5:45 & 8:34	Partly cloudy after 5:30 UT.	1130	89 to 94, 96-98, 100-01-27.
Dec. 26, 2:01 to 3:29	Cirrus clouds at the end.	1137	140-44-47-48-51.
Dec. 30, 3:58 to 5:40	Haze, partly cloudy.	1138	188-92-95-99.
1958			
Jan. 1, 4:58 to 6:18	Strong South wind.	1139	11-13-16-20.
Jan. 4, 2:50 to 6:16	Very strong North-East wind, seeing poor, very clear night.	1139	282-85, 287 to 294.
Jan. 14, 2:34 to 3:32	Cirrus clouds and haze, variable extinction.	1142	224-27-32.
Jan. 23, 2:35 to 5:22	High cirrus clouds, variable extinction.	1145	103-06-09-13-15-22-25-32.

1959ApJS....4..157A

Table 17

Normal points : AO Cass. - BD + 47° 50.

No. of points	Serial numbers	Heliocentric phase in days	$\theta - \theta_o$ degrees	Yellow Δm	Yellow L	Blue Δm	Blue L	Ultra-violet Δm	Ultra-violet L	$\Delta(B_\ell - V_\ell)$	$\Delta(U_\ell - B_\ell)$
4	315 & 1 to 3	0.018	008.64	0.334	0.8678	0.284	0.8662	- 0.261	0.8614	- 0.050	- 0.545
4	4 to 7	0.133	020.39	0.307	0.8896	0.264	0.8823	- 0.289	0.8839	- 0.042	- 0.554
4	8 to 11	0.185	025.70	0.306	0.8904	0.242	0.9003	- 0.304	0.8962	- 0.065	- 0.546
4	12 to 15	0.218	029.07	0.294	0.9003	0.248	0.8954	- 0.295	0.8888	- 0.046	- 0.545
4	16 to 19	0.241	031.42	0.279	0.9129	0.224	0.9154	- 0.316	0.9061	- 0.054	- 0.541
4	20 to 23	0.260	033.36	0.270	0.9204	0.221	0.9179	- 0.326	0.9145	- 0.050	- 0.547
3	24 to 26	0.302	037.66	0.264	0.9256	0.211	0.9264	- 0.338	0.9247	- 0.053	- 0.549
4	27 to 30	0.350	042.56	0.252	0.9358	0.201	0.9350	- 0.348	0.9333	- 0.052	- 0.549
4	31 to 34	0.400	047.67	0.234	0.9515	0.192	0.9428	- 0.373	0.9550	- 0.042	- 0.565
4	35 to 37 & 41	0.457	053.49	0.221	0.9629	0.173	0.9594	- 0.386	0.9665	- 0.048	- 0.559
4	38 to 40 & 42	0.472	055.02	0.234	0.9515	0.193	0.9419	- 0.354	0.9384	- 0.041	- 0.547
4	43 to 46	0.504	058.29	0.233	0.9524	0.182	0.9515	- 0.372	0.9541	- 0.052	- 0.553
4	47 to 50	0.536	061.56	0.228	0.9568	0.178	0.9550	- 0.364	0.9471	- 0.050	- 0.541
4	51 to 54	0.566	064.63	0.229	0.9559	0.171	0.9612	- 0.378	0.9594	- 0.058	- 0.549
4	55 to 57 & 59	0.604	068.51	0.237	0.9489	0.181	0.9524	- 0.378	0.9594	- 0.056	- 0.561
4	61-63-65-67	0.641	072.29	0.217	0.9665	0.164	0.9674	- 0.388	0.9683	- 0.052	- 0.552
4	69-72-74-76	0.686	076.89	0.214	0.9692	0.169	0.9629	- 0.395	0.9745	- 0.044	- 0.564
3	58-60-62	0.622	070.35	0.195	0.9863	0.147	0.9827	- 0.395	0.9745	- 0.048	- 0.542
4	64-66-68-70	0.654	073.62	0.192	0.9890	0.148	0.9817	- 0.400	0.9790	- 0.044	- 0.548
4	71-73-75-77	0.690	077.30	0.197	0.9845	0.144	0.9854	- 0.403	0.9817	- 0.052	- 0.552
4	78 to 81	0.723	080.67	0.192	0.9890	0.142	0.9872	- 0.410	0.9881	- 0.050	- 0.554
4	82 to 85	0.759	084.35	0.186	0.9945	0.136	0.9927	- 0.418	0.9954	- 0.049	- 0.555
4	86 to 89	0.800	088.54	0.182	0.9982	0.132	0.9963	- 0.420	0.9972	- 0.050	- 0.552
3	90 to 92	0.847	093.34	0.194	0.9872	0.146	0.9836	- 0.406	0.9845	- 0.047	- 0.553
4	93 to 96	0.888	097.53	0.202	0.9799	0.150	0.9799	- 0.400	0.9790	- 0.052	- 0.550
4	97 to 100	0.920	100.80	0.208	0.9745	0.158	0.9727	- 0.387	0.9674	- 0.050	- 0.545
4	101 to 104	0.950	103.86	0.208	0.9745	0.168	0.9638	- 0.374	0.9559	- 0.040	- 0.541
4	105 to 108	0.976	106.52	0.198	0.9836	0.162	0.9692	- 0.382	0.9629	- 0.034	- 0.544
4	109 to 112	0.993	108.25	0.214	0.9692	0.171	0.9612	- 0.371	0.9532	- 0.042	- 0.546
4	113 to 116	1.009	109.89	0.225	0.9594	0.172	0.9603	- 0.386	0.9665	- 0.054	- 0.557
4	117 to 120	1.028	111.83	0.231	0.9541	0.194	0.9410	- 0.371	0.9532	- 0.038	- 0.564
4	121 to 124	1.040	113.06	0.240	0.9462	0.187	0.9471	- 0.347	0.9324	- 0.052	- 0.534
4	125 to 128	1.054	114.49	0.234	0.9515	0.185	0.9489	- 0.353	0.9376	- 0.049	- 0.538
4	129 to 132	1.068	115.92	0.242	0.9445	0.195	0.9402	- 0.341	0.9273	- 0.046	- 0.536
4	133 to 136	1.083	117.45	0.252	0.9358	0.202	0.9341	- 0.338	0.9247	- 0.051	- 0.539
4	137 to 140	1.110	120.21	0.245	0.9419	0.205	0.9315	- 0.344	0.9298	- 0.040	- 0.550
4	141 to 144	1.134	122.66	0.249	0.9384	0.204	0.9324	- 0.334	0.9213	- 0.046	- 0.537
4	145 to 148	1.154	124.70	0.262	0.9273	0.212	0.9256	- 0.333	0.9204	- 0.051	- 0.545
4	149 to 152	1.178	127.16	0.265	0.9247	0.218	0.9204	- 0.326	0.9145	- 0.047	- 0.544
4	153 to 156	1.366	146.36	0.326	0.8742	0.275	0.8734	- 0.277	0.8742	- 0.051	- 0.552
4	157 to 160	1.397	149.53	0.330	0.8710	0.278	0.8710	- 0.267	0.8662	- 0.052	- 0.545
4	161 to 164	1.422	152.09	0.327	0.8734	0.282	0.8678	- 0.266	0.8654	- 0.045	- 0.548

1959ApJS....4..157A

Table 17 (continued)

No. of points	Serial numbers	Heliocentric phase in days	$\hat{l} - \theta_o$ degrees	Yellow Δm	Yellow L	Blue Δm	Blue L	Ultra-violet Δm	Ultra-violet L	$\Delta(B_\ell - V_\ell)$	$\Delta(U_\ell - B_\ell)$
4	165 to 168	1.454	155.35	0.327	0.8734	0.291	0.8606	- 0.252	0.8543	- 0.036	- 0.543
3	169 to 171	1.536	163.73	0.340	0.8630	0.294	0.8582	- 0.241	0.8457	- 0.046	- 0.536
4	173 to 176	1.578	168.02	0.348	0.8566	0.296	0.8566	- 0.243	0.8472	- 0.054	- 0.536
4	177 to 180	1.603	170.58	0.358	0.8488	0.306	0.8488	- 0.221	0.8302	- 0.052	- 0.527
4	181 to 184	1.631	173.44	0.348	0.8566	0.300	0.8535	- 0.250	0.8527	- 0.048	- 0.550
4	185 to 188	1.664	176.81	0.349	0.8559	0.311	0.8449	- 0.232	0.8387	- 0.038	- 0.543
4	189 to 192	1.691	179.57	0.352	0.8535	0.306	0.8488	- 0.238	0.8433	- 0.046	- 0.544
4	193 to 196	1.714	181.92	0.336	0.8662	0.290	0.8614	- 0.260	0.8606	- 0.046	- 0.550
3	197 to 199	1.738	184.37	0.346	0.8582	0.284	0.8662	- 0.255	0.8566	- 0.062	- 0.539
3	200 to 202	1.840	194.79	0.314	0.8839	0.245	0.8978	- 0.280	0.8766	- 0.069	- 0.525
3	203 to 205	2.034	214.61	0.264	0.9256	0.203	0.9333	- 0.341	0.9273	- 0.061	- 0.544
3	206 to 208	2.077	219.01	0.242	0.9445	0.198	0.9376	- 0.360	0.9436	- 0.044	- 0.557
4	209 to 212	2.154	226.87	0.221	0.9629	0.174	0.9585	- 0.375	0.9568	- 0.047	- 0.549
4	213 to 216	2.463	258.44	0.204	0.9781	0.154	0.9763	- 0.402	0.9808	- 0.050	- 0.556
4	217-18-20-22	2.498	262.02	0.202	0.9799	0.163	0.9683	- 0.394	0.9736	- 0.040	- 0.557
4	226-28-30-33	2.558	268.15	0.208	0.9745	0.150	0.9799	- 0.432	1.0084	- 0.058	- 0.582
4	234-36-38-39	2.594	271.83	0.200	0.9817	0.150	0.9799	- 0.407	0.9854	- 0.050	- 0.558
4	240 to 243	2.625	275.00	0.207	0.9754	0.150	0.9799	- 0.400	0.9790	- 0.057	- 0.550
4	244 to 247	2.658	278.37	0.210	0.9727	0.150	0.9799	- 0.419	0.9963	- 0.060	- 0.570
4	219-21-23-24	2.513	263.55	0.174	1.0055	0.116	1.0111	- 0.444	1.0196	- 0.058	- 0.560
3	225-27-29	2.545	266.82	0.175	1.0046	0.115	1.0120	- 0.424	1.0009	- 0.060	- 0.539
4	231-32-35-37	2.575	269.89	0.176	1.0037	0.124	1.0037	- 0.405	0.9836	- 0.053	- 0.528
4	248 to 251	2.729	285.62	0.193	0.9881	0.153	0.9972	- 0.403	0.9817	- 0.040	- 0.556
4	252 to 255	2.764	289.20	0.201	0.9808	0.148	0.9817	- 0.420	0.9972	- 0.053	- 0.568
4	256 to 259	2.790	291.85	0.206	0.9763	0.160	0.9710	- 0.410	0.9881	- 0.046	- 0.570
4	260 to 263	2.818	294.71	0.214	0.9692	0.156	0.9745	- 0.416	0.9936	- 0.057	- 0.572
4	264 to 267	2.874	300.43	0.218	0.9656	0.173	0.9594	- 0.417	0.9945	- 0.045	- 0.590
4	268 to 271	3.000	313.31	0.267	0.9230	0.216	0.9221	- 0.309	0.9003	- 0.051	- 0.526
4	272 to 275	3.036	316.99	0.280	0.9120	0.225	0.9145	- 0.320	0.9095	- 0.056	- 0.544
4	276 to 279	3.075	320.97	0.288	0.9053	0.239	0.9028	- 0.305	0.8970	- 0.048	- 0.544
4	280 to 283	3.106	324.14	0.285	0.9078	0.239	0.9028	- 0.313	0.9036	- 0.046	- 0.552
4	284 to 287	3.130	326.59	0.296	0.8987	0.247	0.8962	- 0.295	0.8888	- 0.049	- 0.542
4	288 to 291	3.182	331.90	0.305	0.8913	0.261	0.8847	- 0.282	0.8782	- 0.044	- 0.543
3	292 to 294	3.240	337.83	0.323	0.8766	0.283	0.8670	- 0.264	0.8638	- 0.041	- 0.547
4	295 to 298	3.352	349.27	0.337	0.8654	0.283	0.8670	- 0.272	0.8702	- 0.054	- 0.556
4	299 to 302	3.401	354.28	0.342	0.8614	0.288	0.8630	- 0.270	0.8686	- 0.054	- 0.558
4	303 to 306	3.442	358.47	0.354	0.8519	0.297	0.8559	- 0.245	0.8488	- 0.057	- 0.542
4	307 to 310	3.463	000.61	0.351	0.8543	0.298	0.8551	- 0.250	0.8527	- 0.053	- 0.551
4	311 to 314	3.494	003.78	0.347	0.8574	0.292	0.8598	- 0.252	0.8543	- 0.056	- 0.544
Probable errors				0.005		0.005		0.008		0.003	0.005

The light-curve outside the eclipses was represented for all three colors by means of an expression of the form:

$$L = A_0 + A_1 \cos(\theta - \theta_0) + A_2 \cos 2(\theta - \theta_0) + A_3 \cos 3(\theta - \theta_0) + B_1 \sin(\theta - \theta_0) + B_2 \sin 2(\theta - \theta_0) + B_3 \sin 3(\theta - \theta_0) .$$

The coefficients of the trigonometric terms, obtained graphically by the method of Russell and Merrill (1952), are listed in Table 18; their probable errors are of the order of 0.0010 on the basis of the fit for normal points. Table 18 also gives the interval of primary eclipse estimated from the graphs. As noted by previous authors, although the ellipticity term in cos 2θ is dominant, the asymmetric terms in sin θ and sin 2θ are also quite substantial. Even the terms in sin 3θ and cos 3θ are not entirely negligible. Further, the coefficient of the reflection term in cos θ is positive or zero, which in all cases cor-

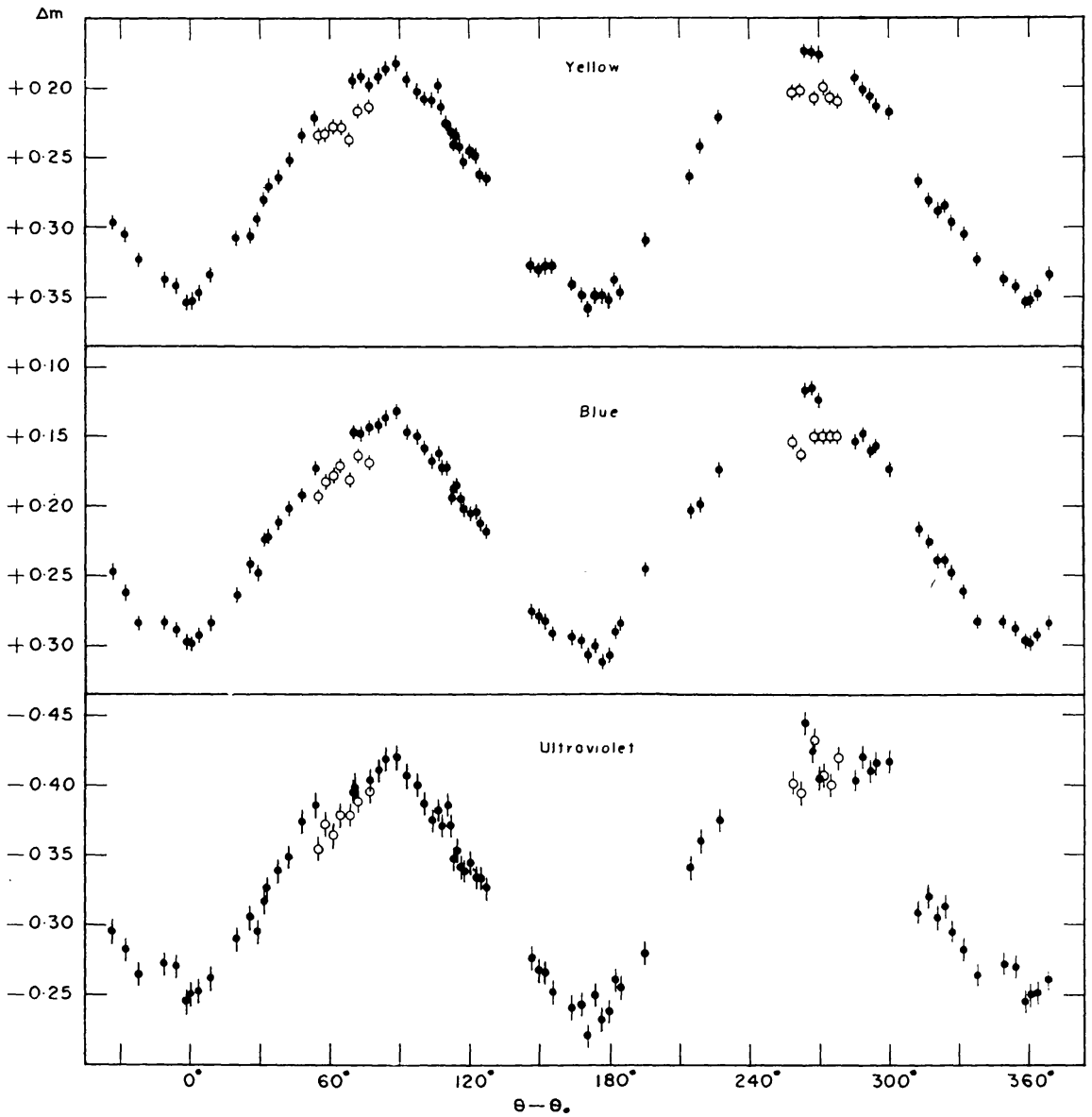

FIG. 11.—The light-curves for AO Cassiopeiae. The open circles at phases 60° and 270° represent observations of September 7 and September 16, 1957, respectively.

1959ApJS....4..157A

Table 18

Representation of light curves of AO Cassiopeiae.

Term / Color	Constant Ao	Cos(θ-θo) A1	Cos 2(θ-θo) A2	Cos 3(θ-θo) A3	Sin(θ-θo) B1	Sin 2(θ-θo) B2	Sin 3(θ-θo) B3	Interval of primary eclipse
V_ℓ	+ 0.9305	0.0000	- 0.0665	- 0.0021	- 0.0099	+ 0.0170	- 0.0029	± 16°
B_ℓ	+ 0.9280	+ 0.0020	- 0.0680	- 0.0018	- 0.0113	+ 0.0182	- 0.0023	± 13°
U_ℓ	+ 0.9265	+ 0.0043	- 0.0695	- 0.0022	- 0.0140	+ 0.0174	- 0.0032	± 14°

responds to a negative reflection. On account of these complications, for which there is no satisfactory theory at present, a new orbit was not computed specifically, since solutions obtained by symmetrizing the light-curve are already available from the works of Pearce, Wood, and Dadaev.

The quantities A_0, A_1, A_2, and B_1 seem to vary from visual to ultraviolet light; simultaneous observations in the red region will be more useful in detecting differences with wave length. The observed colors are essentially constant throughout the whole period, but there is a small diminution of ultraviolet light, about 0.01 mag. at secondary eclipse, and a slight excess of about 0.01 mag. at the maximum following it. In the region of the eclipse the observed points lie only about 0.01 mag. below the curve computed on the basis of observations outside the eclipse. This indicates extremely shallow eclipses, even shallower than the depth of the eclipses found by other authors.

The observed shift of the primary minimum, which is -0.067 day, can be compared with the shifts of -0.06 and -0.1 day found by Hiltner (1949) and by Dadaev (1954), respectively. But observations made after 1928 cannot be represented by a single period. Moreover, the time of the primary eclipse computed from the present spectroscopic orbit falls 0.1 day ahead of the observed primary minimum of light, while the eclipse computed from the spectroscopic orbit by Struve and Horak occurs 0.04 day before the primary minimum observed by Hiltner. Perhaps, as suggested by Dadaev, the presence of masses of gas in the system might be affecting times of minima and the shape of the light-curve.

X. CONCLUDING REMARKS

During the last two decades the role of dynamical interaction and exchange of mass between the components of close binaries in modifying the course of their evolution has become more and more apparent. More recently it is suspected that the nova phenomenon might be connected with the binary character of stars. But no general evolutionary picture has yet emerged from the mass of available data. As mentioned in the introductory paragraphs, the present work was undertaken to obtain more information about close binaries at various stages of evolution; but the material obtained has failed to provide clues regarding any general trends. All the three binaries that were observed indicate that detached masses of gas are present in the systems. Beyond this a more meaningful interpretation is not possible at the present time.

However, we have obtained one important result which has bearing upon the internal structure of early-type stars. Apsidal motion in β Sco and AO Cas is of considerable interest from the point of view of checking the theoretical models of massive stars. Observations give $\log k = -2.6$, or $n_{\text{eff}} = 3.7$, for β Sco, and $\log k = -3.2$, or $n_{\text{eff}} = 4.2$ for AO Cas. The masses of individual components lie between 10 and 20 solar masses. Therefore, the theoretical results have to be interpolated between those for the largest mass ($10\ \mathfrak{M}_\odot$) considered by Kushwaha (1957) and the smallest mass ($28\ \mathfrak{M}_\odot$) considered by Schwarzschild and Härm (1958). The latter authors do not give n_{eff} for their models; but from the tabulated values of $R/R_\odot$ and ρ_c we obtain $n_{\text{eff}} = 2.5$ for the initial model and $n_{\text{eff}} = 4.1$ for the model with the age of 6×10^6 years. The same procedure gives n_{eff} 2.6 and 3.6 for Kushwaha's models with zero age and the age of 34×10^6 years, respectively. From the integrations of the models he had obtained $n_{\text{eff}} = 2.8$ and 3.1 for the same two models. Therefore, n_{eff} should be more like 3.5 in the case of the model for $28\ \mathfrak{M}_\odot$ at the age of 6×10^6 years. It appears that the theoretical models are less centrally condensed than the observations would indicate, and this is so even for the models corresponding to the advanced stages of evolution. The discrepancy is in the same direction as for the binaries considered by Kushwaha; the more recent models by Henyey, LeLevier and Levee (1959) do not improve the situation.

I am grateful to Professor O. Struve for his guidance and encouragement throughout the course of this work and for the use of his and Dr. J. Sahade's Mount Wilson plates. I am indebted to Dr. S.-S. Huang and Dr. Sahade for many stimulating discussions, to Dr.

Huang for his assistance with the IBM 701 computations, and to Professor L. G. Henyey for allowing me computer time. Finally, it is a pleasure to record my appreciation to Dr. C. D. Shane, director of the Lick Observatory, for extending to me the use of the Observatory facilities, and to thank the Regents of the University of California for the grant of Lick fellowships for the period 1955–1958.

REFERENCES

Abhyankar, K. D. 1957, *Pub. A.S.P.*, **69**, 385.
Abhyankar, K. D., and Spinrad, Hyron. 1958, *Pub. A.S.P.*, **70**, 411.
Adams, W. S., and Stromberg, G. 1918, *Ap. J.*, **47**, 329.
Bennett, A. L. 1938, *A.J.*, **47**, 104.
Binnendjik, L. 1952, *Ap. J.*, **115**, 446.
Blaauw, A. 1946, *Groningen Pub.*, No. 52.
Dadaev, A. N. 1954, *Izvestia Pulkovo*, **19**, 31.
Daniel, Z., and Schlesinger, F. 1912, *Alleghany Obs. Pub.*, **2**, 127.
Duncan, J. C. 1912, *Lowell Obs. Bull.*, **2**, 21.
Güssow, M. 1929, *A.N.*, No. 5683.
Guthnick, P. 1920, *A.N.*, No. 5061.
———. 1923*a*, *Vierteljahrschr. Astr. Gesellsch.*, **58**, 83.
———. 1923*b*, *Atti Pontif. Accad. Romana Nouvi Lincei*, Vol. **76**, sessio VI, May 20.
Guthnick, P., and Pavel, F. 1921, *A.N.*, No. 5156.
Henyey, L. G., LeLevier, R., and Levee, L. D. 1959, *Ap. J.* **129**, 2.
Hiltner, W. A. 1949, *Ap. J.*, **110**, 443.
———. 1956, *Ap. J. Suppl.*, Vol. **2**, No. 24.
Hogg, A. R., and Kron, G. E. 1955, *A.J.*, **60**, 365.
Inglis, S. J. 1956, *Pub. A.S.P.*, **68**, 259.
Kuiper, G. P. 1935, *Pub. A.S.P.*, **47**, 15.
———. 1941. *Ap. J.*, **93**, 133.
Kushwaha, R. S. 1957, *Ap. J.*, **125**, 242.
Luyten, W. J., Struve, O., and Morgan, W. W. 1940, *Yerkes Obs. Pub.*, **7**, 264.
McCuskey, S. W. 1956, *Ap. J.*, **123**, 464.
Moore, J. H., and Neubauer, F. J. 1948, *Lick Obs. Bull.*, **20**, 1.
Morgan, W. W., Whitford, A. E., and Code, A. D. 1953, *Ap. J.*, **118**, 318.
———. 1955, *Ap. J. Suppl.*, Vol. **2**, No. 14.
Münch, G. 1957, *Ap. J.*, **125**, 56.
Pearce, J. A. 1926, *Pub. Dom. Ap. Obs. Victoria*, **3**, 275.
Petrie, R. M. 1939, *Pub. Dom. Ap. Obs. Victoria*, **7**, 205.
———. 1950, *ibid.*, **8**, 319.
Plaskett, J. S. 1922, *Pub. Dom. Ap. Obs., Victoria*, **2**, 147.
Russell, H. N. 1939, *Ap. J.*, **90**, 641.
Russell, H. N., and Merrill, J. E. 1952, *Princeton Contr.*, No. **26**, p. 54.
Sahade, J., Huang, S.-S., Struve, O., and Zebergs, V. 1959, *Trans. Amer. Phil. Soc.*, Vol. **49**, Part 1.
Schwarzschild, M., and Härm, R. 1958, *Ap. J.*, **128**, 348.
Slettebak, A. 1956, *Ap. J.*, **124**, 173.
Slipher, V. M. 1903, *Lowell Obs. Bull.*, **1**, 4.
Stebbins, J. 1914, *Ap. J.*, **39**, 481.
———. 1928, *Pub. Washburn Obs.*, **15**, 76.
Sterne, T. E. 1941, *Proc. Nat. Acad. Sci.*, **27**, 175.
Stone, S. N. 1956, Berkeley thesis.
Struve, O. 1937, *Ap. J.*, **85**, 41.
———. 1941, *ibid.*, **93**, 104.
———. 1948, *ibid.*, **107**, 327.
Struve, O., and Horak, H. G. 1949, *Ap. J.*, **110**, 447.
Struve, O., Sahade, J., and Huang, S.-S. 1958, *Ap. J.*, **127**, 148.
Struve, O., Sahade, J., Huang, S.-S., and Zebergs, V. 1958, *Ap. J.*, **128**, 310.
Trefftz, E., Schlüter, A., Dettmar, K.-H., and Jörgens, K. 1957, *Zs. f. Ap.*, **44**, 1.
Traving, G. 1957, *Zs. f. Ap.*, **41**, 215.
Underhill, A. B. 1951, *Canadian J. Phys.*, **29**, 447.
———. 1951*a*, *Pub. Dom. Ap. Obs. Victoria*, **8**, 357.
Unsöld, A. 1941, *Zs. f. Ap.*, **21** 1.
———. 1955, *Physik der Sternatmosphären* (Berlin: Springer Verlag).
Wellmann, P. 1952, *Zs. f. Ap.*, **30**, 71.
Wood, F. B. 1948, *Ap. J.*, **108**, 28.